

Microorganisms and Functional Genes Associated with Cometabolic Degradation of 1,4-Dioxane in Biologically-Active Carbon Biofilters Applied for Potable Reuse Treatment

Katherine Scott

Thesis submitted to the faculty of the Virginia Polytechnic Institute and State University  
in partial fulfillment of the requirements for the degree of

Master of Science

In

Environmental Sciences and Engineering

Amy J. Pruden, Chair

Charles B. Bott

Mark A. Widdowson

March 1<sup>st</sup>, 2024

Blacksburg, VA

Keywords: Metagenomics, Biofiltration, Potable Reuse

# Microorganisms and Functional Genes Associated with Cometabolic Degradation of 1,4-Dioxane in Biologically Active Carbon Biofilters Applied for Potable Reuse Treatment

Katherine Scott

## ABSTRACT

1,4-dioxane is a probable human carcinogen frequently found in water and wastewater systems at concentrations above the EPA one-in-one-million cancer risk level of 0.35 ug/L. 1,4-dioxane is not well removed through conventional treatment methods due to its polarity and resistance to biodegradation, especially when present at low ( $\mu\text{g/L}$ ) concentrations. Cometabolic degradation of 1,4-dioxane has been achieved in groundwater remediation by stimulating bacteria carrying cyclic ether-degrading soluble diiron monooxygenases (SDIMOs) through the addition of simple alkane gases, such as propane. A recent pilot-scale study demonstrated that addition of such co-substrates prior to biological active filtration (BAF) holds potential as a novel potable reuse treatment approach that can effectively remove 1,4-dioxane.

Characterization of the microbial communities associated with propane-induced cometabolism of 1,4-dioxane has largely been limited to culture or polymerase chain reaction (PCR)-dependent methods, which are highly limited in throughput, generally providing information about one organism or one gene at a time. Shotgun metagenomic sequencing is a high-throughput nontargeted means of broadly profiling microbial taxa and functional genes involved in various metabolic processes. In this thesis, methods for DNA extraction from granular activated carbon applied to full-scale BAF amended with propane for the purpose of 1,4-dioxane cometabolism were optimized and metagenomic sequencing was performed. Insights were gained into the microbes and functional genes involved in 1,4-dioxane biodegradation, furthering our understanding of a potentially powerful new water reuse treatment technology that effectively polishes recalcitrant contaminants.

# Microorganisms and Functional Genes Associated with Cometabolic Degradation of 1,4-Dioxane in Biologically Active Carbon Biofilters Applied for Potable Reuse Treatment

Katherine Scott

## GENERAL AUDIENCE ABSTRACT

Water reuse systems use advanced wastewater treatment technologies to treat wastewater to such high standards that it can even be used as a source for drinking water. Expanding water reuse is a vital means of protecting water resources, but the treatments can be very costly. Biofiltration is a reuse treatment technology in which water is filtered through media - such as activated carbon - that is commonly used in household filtration systems, providing surface area for the growth of beneficial microorganisms that can naturally biodegrade contaminants in the water. Some contaminants are more difficult to degrade than others, especially trace levels of pharmaceuticals and personal care products. One common manufacturing ingredient that ends up in wastewater and is difficult to biodegrade is 1,4-dioxane, a compound that is potentially carcinogenic to humans at  $\mu\text{g/L}$  concentrations when consumed via drinking water over a lifetime.

It was recently discovered that adding propane to a biofilter can help to improve biodegradation of 1,4-dioxane down to very low levels. Propane acts as a co-metabolite, i.e., providing a food source on which 1,4-dioxane-degrading bacteria can thrive. In this study, DNA sequencing technology was applied to help identify the bacteria that are responsible for co-metabolic degradation of 1,4-dioxane in a granular activated carbon biofilter. The research was conducted at a demonstration-scale research facility that is investigating innovative ways to treat wastewater to levels that are suitable for recharging a groundwater aquifer that is used as a drinking water source. The main contributions of this study include an optimized protocol for obtaining DNA from the BAF media for DNA sequencing and new insight into the bacteria and enzymes involved in co-metabolic degradation of 1,4-dioxane.

## Acknowledgements

First and foremost, thank you to my parents, and to my sister for giving me two very cute nieces (hi Maddie and Hailey) in my time here who I look forward to spending more time with very soon. Thanks to my grandmothers for being the best.

Thank you to my advisor, Dr. Pruden, who has trusted me with so much during my time here and has been so relentlessly encouraging and patient and has helped me realize my full potential. Thank you also to my committee, Dr. Charles Bott and Dr. Mark Widdowson, for your extremely valuable time and consideration. I'm also grateful for the generous funding provided by HRSD, USBR, and the NSF-NRT, and for the students, engineers, operators, and staff at the SWIFT Research Center (especially Hannah) for making this research possible and letting me be a part of this project.

I feel lucky to have worked in such a wonderful lab environment full of intelligent, caring people who constantly offer their help (in the forms of rides home, desk cookies, notes/words of encouragement, plants, coffee, tea, etc.) and ask for little in return, and who make the office/lab a lively place. I'm grateful to know every one of my coworkers – there are too many to name who have each helped me in a remarkable way, so if you're a Prudenian and you're reading this, you're included. Thanks in particular to Matt, who taught me what I know and who laid the foundation for this work while being so encouraging and ready to help along the way, with some major sanity checks. Thanks also to Loc and Connor for helping me through the basics of metagenomics.

Thank you to my friends from Jersey – Mary and Matt especially – for being a phone call away at all times. Thank you to my wonderful current and former roommates, especially Hilary, Adam, Juno, Shahwar, Marianne, my Chasewood family, and the rest of my extended family for making grad school so full of fond memories and for turning Virginia into a second home.

## Table of Contents

CHAPTER 1: Cometabolic 1,4-dioxane biodegradation and its application to biofiltration .....	2
Attributions .....	8
CHAPTER 2: Optimization of DNA Extraction from Biologically-Active Granular Activated Carbon .....	9
Abstract .....	9
2.1 Introduction .....	9
2.2 Methods .....	11
2.3 Results .....	15
2.4 Discussion .....	24
2.5 Conclusion .....	26
CHAPTER 3: Metagenomic Insights into Cometabolic Degradation of 1,4-Dioxane in Propane-Amended Biofilters for Water Reuse .....	27
Abstract .....	27
3.1 Introduction .....	27
3.2 Methods .....	31
3.3 Results .....	33
3.4 Discussion .....	47
References .....	60

## **CHAPTER 1: Cometabolic 1,4-dioxane biodegradation and its application to biofiltration**

Water reuse entails treating wastewater to a higher standard, depending on the reuse application (*Guidelines for Water Reuse*, 2004). In the case of potable reuse applications, typically advanced water treatments (AWT) are necessary to minimize any contaminants of emerging concern (CECs), including pharmaceuticals and personal care products, detergents, chemical stabilizers, and flame retardants which may pose threats to human health (Salimi et al., 2017). There are numerous configurations of AWT, but the most common approach is to employ multiple-barriers of physical and chemical treatment processes. Advanced oxidation processes (AOPs), such as ozone, produce hydroxyl radicals that can kill pathogens and destroy various organic pollutants (Y. Deng & Zhao, 2015). Membrane-based technologies are often implemented as a highly stringent means of removing trace biological and chemical materials from the water. Reverse osmosis is the most stringent membrane technology, with a size cutoff of 1 nm, but it is highly costly (Malaeb & Ayoub, 2011).

As water reuse applications are expanding, more cost-effective technologies are needed that are adaptive to local constraints and opportunities. One water reuse treatment that is gaining attention as a viable alternative to membrane-based treatments is ozone combined with biologically-active filtration (BAF). Ozone-BAF is proving to be an economical means to reduce organic carbon, pathogen, and contaminant levels to concentrations acceptable by drinking water standards (Gerrity et al., 2014; Summers et al., 2020; Sundaram et al., 2020; Vaidya et al., 2020). Still, there is a need to establish the extent to which ozone-BAF-based water reuse systems can reliably remove the array of CECs that can persist in secondary wastewater effluents. One CEC that has been found to be particularly difficult to remove is 1,4-dioxane, a chlorinated solvent stabilizer that can be found in paints, glues, dyes, waxes, greases, cosmetics, detergents and other consumer products (Doherty et al., 2023; Mohr et al., 2020). The U.S. Environmental Protection Agency (US EPA) designated 1,4-dioxane as a probable human carcinogen, with a proposed health-based limit of 0.35 µg/L in drinking water (EPA IRIS, 2013; Mohr et al., 2020). A report under the US EPA Unregulated Contaminant Monitoring Rule reported

1,4-dioxane as the second-most prevalent of the 28 studied UCMR3 contaminants, making it a strong candidate for future regulation (Adamson et al., 2017).

1,4-dioxane is non-volatile and hydrophilic, resulting in its high mobility in water and low adsorption to activated carbon (Otto & Nagaraja, 2007). Due to its unique chemical characteristics and ubiquity at low levels in wastewater, specialized treatment approaches are needed for enhanced removal of 1,4-dioxane to meet potentially strict regulatory limits. 1,4-dioxane removal can be achieved through advanced oxidation processes, which can help to break up organic molecules. However, AOPs are costly and can be challenging to apply in practice to certain water chemistries. For example, while 1,4-dioxane removal via ozonation is dependent on the formation of hydroxyl radicals, other constituents in the water can also react with these radicals to produce harmful by-products such as bromate (Hogard et al., 2021; Vatankhah et al., 2019). 1,4-dioxane is also generally resistant to biodegradation due to its cyclic ether structure, though several studies have reported environmentally sparse bacterial strains that are capable of degrading 1,4-dioxane as a primary substrate (Inoue et al., 2016; Mahendra & Alvarez-Cohen, 2006; Sales et al., 2013). However, one major limitation of these lab studies is the high concentrations of 1,4-dioxane that are required for biodegradation to ensue. Due to its unique chemical characteristics and ubiquity at low levels in wastewater, specialized treatment approaches are needed to achieve effective removal of 1,4-dioxane. This need is especially urgent as some states develop their own drinking water and groundwater standards for 1,4 dioxane below 1 ug/L, such as in Colorado where the groundwater standard is 0.35 ug/L (Colorado DPHE, 2013).

Biofilms that grow on and within media applied in BAFs, such as biological activated carbon (BAC), harbor microbial communities with extensive metabolic potential. A previous study applying shotgun metagenomic sequencing to profile the composition of these diverse microbial communities found enrichment of aromatic degradation genes on BAC media compared to biofilter influent (Oh et al., 2018). However, biofilter-mediated biodegradation of 1,4-dioxane and similar CECs in potable reuse applications is highly limited by low influent concentrations of these contaminants, preventing selection for and activation of rare microorganisms and genes capable of directly metabolizing the target compounds.

Cometabolism offers another means of stimulating biodegradation of recalcitrant micro-level pollutants, such as 1,4-dioxane, on a biofilter. Cometabolism involves the introduction of a primary substrate, ideally a non-toxic one, which at high concentrations stimulates the growth and activation of bacteria and enzymes which degrade not only the primary substrate, but also the trace organic contaminant of interest. Degradation of the contaminant typically does not contribute to generation of biomass or energy for the responsible microbes, but rather occurs as a fortuitous side-reaction as a result of enzyme compatibility with the co-substrate (Dalton et al., 1997). This ultimately results in the complete utilization of the dosed primary substrate as well as enhanced removal of the low-level target contaminant, potentially to sub-parts-per-trillion levels (Hazen, 2018).

The enzymes most frequently involved in aerobic biodegradation of recalcitrant organic contaminants are the oxygenases, which incorporate dioxygen molecules into hydrocarbons and are effective in destabilizing aromatic and aliphatic carbon-carbon bonds (Fuchs et al., 2011). Among these, the soluble di-iron monooxygenases (SDIMOs, also referred to as bacterial multicomponent monooxygenases or BMMs) have been recognized for their common ability to transform a variety of organic contaminants through cometabolism due to their broad substrate range (Leahy et al., 2003; Notomista et al., 2003). SDIMOs are multicomponent enzymes consisting of four to six subunits which coordinate the hydroxylation or epoxidation of aliphatic and aromatic molecules using a dioxygen molecule and NADPH as cofactors (Leahy et al., 2003). The four conserved subunits of SDIMOs consist of the alpha subunit (which contains a carboxylate-stabilized di-iron site responsible for hydroxylation of the substrate), the beta subunit (which coordinates with the alpha subunit to form the overall hydroxylase component), the N subunit (containing a ferredoxin-like N-terminal domain and an NADPH-binding C-terminal domain), and the R subunit (which channels electrons from the oxidation of NADPH to hydroxylation of the substrate) (Leahy et al., 2003; Notomista et al., 2003). Some SDIMO subtypes also contain a variable gamma subunit, which coordinates with the alpha and beta subunits, and/or an extra ferredoxin-like subunit. SDIMOs have been categorized into 6 subgroups based on their alpha subunit amino acid sequence similarity and patterns in their overall structure (i.e., number and

arrangement of subunits, which corresponds to the number and arrangement of genes in the MO operon) (Coleman et al., 2006; Leahy et al., 2003; Notomista et al., 2003).

The sequence-based distinction of these six subgroups somewhat correlates with each group's observed substrate preference (Figure 1.1, Table 1.1). For example, Groups 1 and 2 diverge from the other groups and consist of enzymes which primarily oxidize aromatics (the toluene monooxygenases and phenol hydroxylases, respectively), while groups 3 through 6 are more well-documented for their oxidation of alkanes and alkenes (including methane, propane, butane, ethane, propene, ethene, and other gaseous hydrocarbons) (Holmes, 2009). The alpha subunit is thought to be the subunit that primarily determines substrate specificity and regio/stereo-specificity of the oxidation reaction. This is because the alpha subunit contains the active site, which includes two conserved di-iron-binding DE\*RH domains which coordinate the substrate and the dioxygen molecule. Certain residues near the active site likely play a substantial role in "gating" the substrate docking site, resulting in wider or narrower substrate ranges. For example, a single amino acid substitution (valine to alanine) in the alpha subunit of a toluene monooxygenase derived from *Burkholderia cepacian* G4 resulted in significantly faster degradation of bulky aromatics such as naphthalene (Canada et al., 2002). Manufacturing industries have taken advantage of these functionally important sites to engineer enzymes which specifically oxidize substrates to produce the desired epoxide/enantiomer (Nichol et al., 2015).

Oxygenase genes associated with aromatic catabolism (e.g., SDIMOs, dioxygenases, Rieske non-heme iron monooxygenases, hydroxylases) have been primarily observed in the phyla Actinomycetes and Proteobacteria through both sequence-based screening of putative degradation genes and culture observations (Pérez-Pantoja et al., 2010). However, as with other families of oxygenases implicated in biodegradation, SDIMOs do not exhibit a strong phylogenetic relationship with their host bacteria past the phylum level (e.g., SDIMO protein sequence identity does not match overall genomic or 16S sequence identity between different host species). This observation suggests that horizontal gene transfer of SDIMO gene clusters is a mechanism contributing to the spread and diversification of this gene family (Vilchez-Vargas et al., 2010). Cometabolism is therefore likely not carried out by unique taxa, but rather may be

performed by a number of functionally redundant taxa that might co-exist within a diverse microbial community. SDIMOs are also naturally found in a wide variety of environments throughout the world, including soils and marine sediments, Arctic groundwater, and biofilters (Lee et al., 2021; M. Li et al., 2013). While diverse SDIMOs (from all six subfamilies) can be found in many environments, some may be more prevalent than others. In one environmental study, for example, a notable proportion of sequenced clones (17 of 45) from nested PCR represented genes similar to the alpha subunit of propane monooxygenase (prmA) (Coleman et al., 2006).

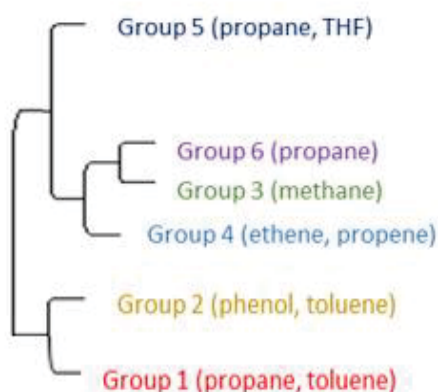


**Figure 1.1** Phylogeny of SDIMO subgroups.

**Table 1.1** Summary of SDIMO subgroups and their most frequently associated substrates.

Group	Primary target?	Frequently associated substrates
Group 1	Aromatics	toluene, propene, benzene
Group 2	Aromatics	phenol, substituted aromatics
Group 3	Aliphatics	methane, butane
Group 4	Aliphatics	ethene, propene, alkenes
Group 5	Aliphatics	propane, THF
Group 6	Aliphatics	propane

Propane monooxygenases (prMOs) and closely related MOs have been implicated in the cometabolism of dioxane, N-Nitrosodimethylamine, cyclohexane, trichloroethylene, vinyl chloride, benzene, toluene, and other recalcitrant hydrocarbons

upon provision of propane as a primary substrate (D. Deng et al., 2018; Polasko et al., 2021; Sales et al., 2013; Sharp et al., 2007; Weidhaas et al., 2012). Propane biosparging has been applied for remediation of groundwater contaminated with 1,4-dioxane and co-occurring chlorinated aliphatics with success (Bell et al., 2022; Chu et al., 2018; Lippincott, 2015). Recently, propane stimulation has shown similar success when applied to biofilters, indicating that biofilter-based cometabolism may be a cost-effective method for treating reuse water to achieve levels of 1,4-dioxane well below the EPA-established health limit (McElroy et al., 2023; Stohr et al., 2023). Biofilter 1,4-dioxane removal in treatment systems with < 1 mg/L influent 1,4-dioxane is limited, with typical removal percentages for biofilters in ozone-BAF systems reported to be below 20% (Vatankhah et al., 2019).

Overall, SDIMOs are a class of widely-distributed enzymes with broad substrate ranges, making them a promising candidate for use in biological water treatment. However, they are not well-studied from an environmental context, and much remains unknown about their potential usefulness in water treatment. This thesis will explore sequencing-based approaches to investigating 1,4-dioxane-cometabolizing microorganisms in biological activated carbon biofilters. Ultimately, this work will answer fundamental questions about which organisms/enzymes are responsible and whether they can provide reliable, cost-effective treatment of water contaminated with ug/L levels of 1,4-dioxane.

The specific objectives of this thesis were to:

1. Optimize protocols for maximizing DNA recovery from BAC biofilters in order to support microbial community analyses via DNA sequencing (Chapter 2)
2. Apply metagenomic sequencing analysis of BAC biofilters employed for potable reuse treatment as a means to identify candidate taxa and functional genes responsible for co-metabolic degradation of 1,4-dioxane via propane amendment (Chapter 3)

### Attributions

The research described herein was performed through support of a partnership between the Hampton Roads Sanitation District (HRSD) Sustainable Water Infrastructure for Tomorrow (SWIFT) and Virginia Tech. HRSD staff, including Dr. Charles Bott, Christopher Wilson, and Germano Salazar, oversaw design and operation of the 1 MGD ozone-BAC-GAC treatment system located at the SWIFT Research Center. The SWIFT ozone-BAC-GAC process treats secondary effluent treated by the Nansemond WWTP to potable reuse standards, recharging the Potomac aquifer. Hannah Stohr, a Virginia Tech PhD student stationed at the SWIFT Research Center, was responsible for the day-to-day operation of the propane-amendment experiments described herein, as well as design of the propane feed system/biofilter cover, safety measures related to the propane system, oversight of construction and startup, and coordination of chemical and microbiological sampling. Dr. Matthew Blair provided guidance in experimental design, especially collection and analysis of samples and the experimental matrix described in Chapter 2. Dr. Amy Pruden advised the overall research project and its implementation. Loc Nguyen and Connor Brown provided crucial guidance for the metagenomic data analysis approach. All sample analysis, data analysis, figure generation, and written description presented in this thesis was carried out by myself, Katherine Scott. Funding was generously provided through the US Bureau of Reclamation, Hampton Roads Sanitation District, and the NSF National Science Foundation Research Traineeship Program at Virginia Tech.

## **CHAPTER 2: Optimization of DNA Extraction from Biologically-Active Granular Activated Carbon**

### Abstract

Granular activated carbon (GAC) filters are widely used as a highly effective water treatment processes in a variety of applications. Over time, GAC filters are colonized with microbes, resulting in a shift from a primarily sorption-driven to a biologically-driven treatment process. This results in conversion of a GAC filter to a biologically-activated carbon (BAC) filter. DNA sequencing could provide new insights into the diverse microbes inhabiting GAC and BAC filters, but is challenged by the strong attachment of biofilms to GAC and the fact that DNA can adhere to the highly sorptive surface of the GAC media. The purpose of this study was to optimize extraction of DNA from GAC/BAC filters to support downstream microbial community analysis. Previously published chemical treatment modifications were compared with several bead beating and sonification modifications to a commercially-available extraction kit when applied to samples of an exhausted GAC filter. High-intensity bead-beating settings were found to increase the yield of DNA by up to 115%, with only mild DNA shearing effects compared to sonication. However, 16S rRNA gene amplicon sequencing of the resulting DNA extracts indicated that higher yields did not significantly affect resulting profiles of the microbial community composition. Increased mechanical lysis through higher-intensity bead-beating may therefore increase the mass of DNA recovered from low-yield activated carbon samples with minimal effect on community composition analysis. Future studies examining the effects of the extraction approaches on microbial community profiles obtained using alternative sequencing technologies, such as metagenomic sequencing or long-read sequencing, would be of value.

### 2.1 Introduction

Granular Activated Carbon (GAC) is a carbon-based medium commonly employed in water treatment trains due to its high capacity for sorption of nonpolar organic contaminants. Purification of water through GAC contacting is primarily considered to be a physical treatment process driven by sorption (L. K. Wang et al., 2004). However, the high surface area and porous structure of GAC allow for the

colonization of microorganisms over time, providing potential for biological removal of organics. Biologically activated carbon (BAC) biofilters make use of this biological component of exhausted GAC to achieve removal of TOC/nutrients and contaminant degradation (Gerrity et al., 2011; Nishijima & Speitel, 2004; L. K. Wang et al., 2004; D. Zhang et al., 2011). In combination with upstream processes such as ozonation, GAC contacting and biofiltration are widely implemented for the purpose of drinking water treatment and now are also beginning to be implemented for water reuse treatment. Understanding the types and functions of microbes that colonize BAC and GAC filters could help to further improve and adapt corresponding treatments for a variety of applications and contexts.

Analysis of DNA recovered from GAC and BAC filters can elucidate the metabolic roles of different microorganisms that inhabit them. Previous studies have conducted 16S rRNA gene amplicon sequencing as a means to profile the microbial communities resident to different types of biofilters and GAC contactors (Camper et al., 1985; Vera et al., 2018; Xu et al., 2023). However, due to its complex structure and high capacity for sorption, GAC presents some challenges for DNA extraction, including strong attachment of the biofilm to the media through production of extracellular polysaccharides (Weber, Jr. et al., 1978) and potential “re-sorbing” of lysed DNA to media after lysis. As a result, previous studies have reported difficulties in obtaining high quality DNA from GAC and BAC media extracts (Babcock et al., 2022; Bacaro et al., 2019). Additionally, the potential for use of GAC in passive environmental DNA samplers has been explored due to its efficiency in free DNA capture, but similar difficulties in extraction were found that ultimately limited its usefulness in this application (Kirtane et al., 2020).

Previous studies have attempted to optimize detachment of biofilms from GAC and BAC media by modifying typical DNA extraction protocols. Tested modifications include shaking/vortexing media in sterile PBS or a “desorption solution” to detach whole cells (Camper et al., 1985; Z. Lu et al., 2020; Zhou et al., 2021), addition of skim milk or Denhardt’s solution as reagents which competitively bind GAC in place of DNA (Takada Hoshino & Matsumoto, 2005; Takada-Hoshino & Matsumoto, 2004; Volossiuk et al., 1995), and sonication (T. G. Kim et al., 2014; Xu et al., 2023). These have been

occasionally applied to extraction of GAC or soil samples with limited success, and have not been compared against one another.

Here, we optimize extraction of microbial DNA from GAC sampled from an exhausted contactor. We initially tested whether sorption of DNA to virgin activated carbon was observable in a bench-scale experiment. We next tested several modifications to a commercial DNA extraction kit (Fast DNA Spin Kit for Soil, MP Bio) including addition of reagents previously reported in GAC extraction optimization literature and alteration of bead-beating steps. We used several metrics to compare final DNA quality and quantity between different extraction modifications. Finally, stratified GAC samples from the top, middle, and bottom of the contactor were extracted with several variations in bead beating settings, and the corresponding microbial communities were compared through 16S rRNA gene amplicon sequencing to evaluate whether the extraction protocol affected the observed microbial communities in each sample.

## 2.2 Methods

### **2.2.1 GAC media collection**

Bulk GAC media was collected in autoclaved polypropylene bottles during emptying of an exhausted GAC contactor at the HRSD SWIFT Research Center in September, 2022. For extraction optimization experiments, a representative sample of the top four inches of the contactor was obtained using an Ekman dredge sterilized with ethanol and washed with GAC effluent. Additional samples were taken from the bottom of the contactor as it emptied, one 9 minutes after emptying began to represent media near the bottom of the exhausted contactor and another taken approximately 10 minutes later to represent media further towards the middle. Collected media was transported to the laboratory on ice within 24 hours of collection, aliquoted into sterile 15 mL Falcon tubes, frozen at -20°C, freeze-dried for 24 hours at -84°C (LabConco FreeZone 4.5 Plus), and ultimately stored at -20°C for future processing. Virgin GAC media (Calgon Corporation Filtrasorb 400) was also collected for use in a kinetic DNA sorption experiment and was stored at -20°C until use.

### 2.2.2 Sorption experiment

To examine the sorption of extracellular DNA to virgin GAC, we obtained DNA extracts from wastewater samples and exposed them to virgin GAC over a 24-hour period. 300 mL of secondary effluent was filtered onto 0.22- $\mu\text{m}$  mixed cellulose ester filters in 18 replicates (S-Pak, Millipore Sigma). Filters were frozen in extraction tubes and extracted using the Fast DNA Spin Kit for Soil (MP Bio, Solon, OH). All 18 extracts were pooled into one tube and quantified through the Qubit dsDNA HS assay and diluted with molecular grade water to a final concentration of 8 ng/ $\mu\text{L}$ . Three groups containing four replicates each were prepared in sterile 1-mL tubes: a control group containing only 500  $\mu\text{L}$  of the diluted DNA extract, a control group containing 200 mg virgin GAC with 500  $\mu\text{L}$  of molecular grade water, and an experimental group containing 200 mg virgin GAC media with 500  $\mu\text{L}$  of the diluted extract. All tubes were briefly vortexed, and a 10  $\mu\text{L}$  “T0” sample was immediately taken from the supernatant of each tube. Tubes were stored in the dark at room temperature, and additional 10  $\mu\text{L}$  samples were taken at times  $t = 3$  mins, 7 mins, 15 mins, 30 mins, 60 mins, 120 mins, and 24 hours after T0. The DNA concentration in each supernatant sample was measured through the Qubit HS DNA assay (Thermo Fisher Scientific Invitrogen, Eugene, OR, CAT Q33231) to monitor the loss of free DNA over time due to sorption.

### 2.2.3 Extraction optimization

#### Test 1: Chemical and physical modifications

All extraction modifications were performed with the Fast DNA Spin Kit for Soil using a FastPrep-24 bead beater (MP Bio, Solon, OH, SKU 116560200-CF) with an input of 200 mg freeze-dried GAC from the top of the exhausted contactor. The typical protocol used for this kit starts with addition of 122  $\mu\text{L}$  MT buffer and 978  $\mu\text{L}$  phosphate buffer to the sample extraction tube, followed by bead-beating for 40 seconds at 6 m/s.

We initially tested two physical and three chemical modifications to DNA extraction previously hypothesized to enhance recovery from GAC. Chemical modifications included addition of 0.05 g/mL skim milk powder (MP) or Denhardt’s solution to the phosphate-MT buffer, which are both thought to competitively bind GAC and allow DNA to remain in the liquid fraction during extraction. Skim milk powder (Millipore-Sigma, CAT 70166) was prepared at a concentration of 0.05 g/mL in Fast

DNA Spin Kit lysis buffer (110  $\mu$ L MT buffer + 889  $\mu$ L sodium phosphate buffer). 10  $\mu$ L molecular grade 100X Denhardt's solution (2% Ficoll type 400, 300mM NaCl, 2% polyvinylpyrrolidone, and 2% bovine serum albumin, G-Biosciences CAT 786-525) was added to 109  $\mu$ L MT buffer and 881  $\mu$ L phosphate buffer from the Fast Spin Kit. A surfactant solution consisting of filter-sterilized Zwittergent 3-12 ( $10^{-6}$  M), EDTA ( $10^{-3}$  M), proteose peptone (100mg/L), and TBS (0.01M, pH 7.0) previously shown to detach cells from GAC was also tested by shaking 200 mg of GAC in 1.5 mL detachment solution for 10 minutes, centrifuging for 8 minutes at 6000 rpm, removing the supernatant, and proceeding with the start of the commercial extraction kit. Controls for the milk powder and cell detachment solutions were also extracted using 200  $\mu$ L of each solution with no added GAC to assess for possible contamination. To evaluate modifications to the physical processes involved in mechanical lysis of GAC-attached cells, we tested bead beating for twice the duration of the recommended bead beating settings (80 seconds). Sonication was also tested due to its theoretical ability to detach DNA from media through aggressive mechanical action. Sonication was performed by submerging the GAC extraction tubes in a bath sonicator (Elmasonic Easy 30/H Ultrasonic Cleaner) for 15 minutes at room temperature after bead beating as per kit protocol and then proceeding with the extraction as normal. Each modification was tested in triplicate alongside triplicate control samples of 200 mg GAC extracted according to the kit protocol with no modifications. Final extract concentrations were measured using the Qubit HS DNA assay. In addition to testing these methods on the exhausted GAC, we attempted to recover sorbed DNA from the virgin GAC used in the initial sorption experiment using each of these modifications.

A second experiment was conducted on the exhausted media to compare several modifications to the kit-specific mechanical lysis protocol, specifically comparing the effect of increasing bead beating duration or speed. Bead beating speeds of 6 m/s, 8 m/s and, 10 m/s were tested on triplicate GAC samples for a duration of 40 seconds. Durations of 80 seconds, 120 seconds, and 180 seconds were also tested at the same speed (6 m/s). An additional three groups were included to test bath sonication for 15 minutes, 30 minutes, and 60 minutes following the manufacturer-recommended bead-beating step. Final extract concentrations were measured through the Qubit DNA assay,

and shearing of DNA was assessed through TapeStation (Agilent Technologies) analysis of these DNA extracts.

To better represent the degree of physical treatment of GAC media in our reporting (taking into account both speed and duration of bead-beating), we devised a metric “intensity-time,” equal to the speed of bead beating (in meters per second) times the duration (in seconds). Samples were therefore processed at intensity-times ranging from 240 m (control samples extracted with 6 m/s for 40 s) to 1080 m (6 m/s for 180 s).

#### **2.2.4 Extraction of stratified GAC samples and 16S rRNA amplicon sequencing**

Stratified GAC samples collected from the nominal “bottom” and “middle” of the contactor were extracted in triplicate using the same range of bead beating settings used in the second modification experiment for comparison to the top-collected samples. 16S rRNA sequences from each extract were amplified in triplicate with a no-template control using barcoded 515F/926R universal primers (Walters et al., 2015). Each 25  $\mu$ L reaction consisted of 1  $\mu$ L GAC extract diluted 1:10, 12.5  $\mu$ L AccuStart II PCR SuperMix (Quantabio, CAT 95137), 10.5  $\mu$ L molecular grade water, and 0.5  $\mu$ L each of 10  $\mu$ M forward and reverse primers. Cycling conditions consisted of 94°C for 3 minutes followed by 30 cycles of 94°C for 45 seconds, 50°C for 60 seconds, and 72°C for 90 seconds, followed by 72°C for 10 minutes and a hold at 4°C. Triplicate amplifications were combined, quantified through the Qubit DNA HS assay, and pooled into a library using 240 ng DNA per sample. The pool was cleaned using the QiaQuick PCR Purification Kit (Qiagen, CAT 28104), purified through Pippin Prep to remove high molecular weight material, and sequenced on a 600 cycle v3 Illumina MiSeq (2 x 150 bp).

#### **2.2.5 Data analysis and statistics**

All amplicon sequencing data processing was performed in QIIME2 (2020.6) (Bolyen et al., 2019). Raw demultiplexed sequences were denoised with DADA2, after which singletons were removed. A classifier trained using the 515F/926R GreenGenes database (v13.5) at 99% clustering was used to classify representative sequences (DeSantis et al., 2006). Mitochondria and chloroplast sequences were removed, and final feature tables were imported into R for statistical analysis. The vegan package was used to generate beta diversity dissimilarity matrices using Bray-Curtis and Jaccard metrics at

the family level, and statistical differences in community composition due to the extraction method and the GAC stratum (top, middle, or bottom) were tested using *adonis2*, not considering independent variable interactions (Oksanen et al., 2022). Posthoc tests were performed with the *pairwiseAdonis* package (Arbizu, 2017). All p-value cutoffs were set at 0.01.

## 2.3 Results

### **2.3.1 Sorption of free DNA to virgin GAC media**

Figure 2.1 illustrates the sorption of free DNA to virgin GAC media over 24 hours. Immediate sorption of free DNA to GAC was observed within three minutes of incubation. Over half of the free DNA appeared to sorb to the virgin GAC within two hours of incubation, and 90% was apparently sorbed after 24 hours, resulting in an estimated DNA concentration of 6-7 ng/ $\mu$ L on the DNA-exposed GAC. Attempting to recover sorbed DNA from the media resulted in yields less than 1 ng/ $\mu$ L DNA using the recommended extraction protocol, the detachment solution method, and the 15-minute sonication modification. DNA yields were highest for milk powder-treated samples (averaging 1.4 ng/ $\mu$ L), but control DNA extracts from the milk powder solution alone yielded up to 4 ng/ $\mu$ L, suggesting that the inflated yield was the result of contamination.

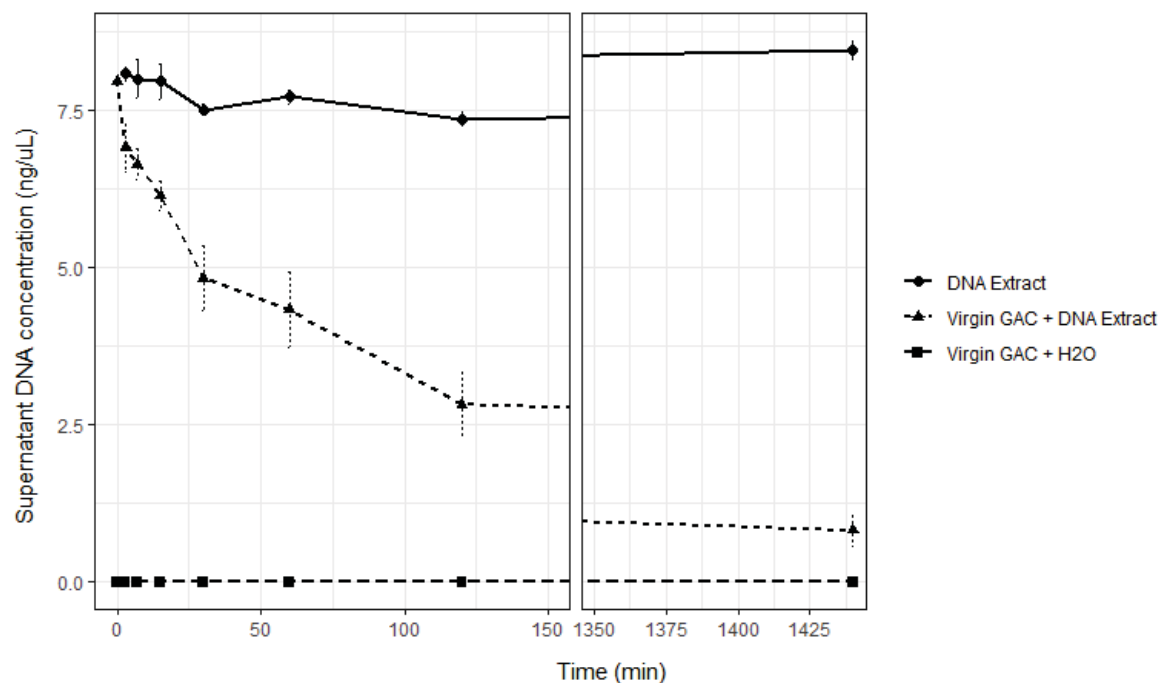


**Figure 2.1.** DNA sorption to GAC was tested by exposing extracellular DNA extracted from secondary wastewater (approximately 8 ng/μL) to 200 mg virgin GAC over 24 hours of incubation at room temperature (“Virgin GAC + DNA Extract”). Controls consisted of tubes containing only the DNA extract (“DNA Extract”) to account for potential DNA degradation at room temperature and tubes containing only virgin GAC with molecular-grade water (“Virgin GAC + H2O”) as a “blank” with no DNA present. Four replicates were tested for each condition. Error bars represent standard deviation.

### 2.3.2 Quantity and quality of DNA extracted from exhausted GAC

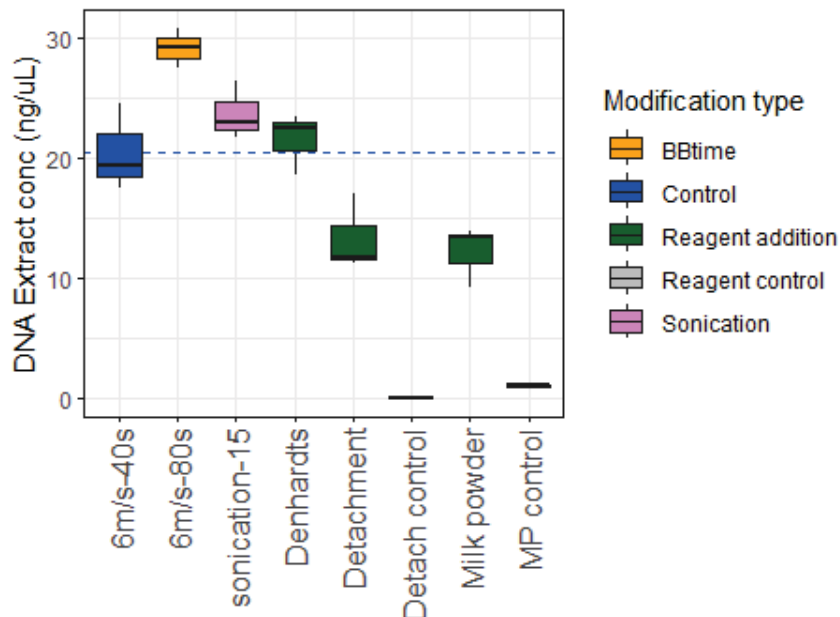
In the first experiment, all three chemical treatments were ineffective in significantly increasing DNA yield relative to the control extract (Figure 2.2). Sonication for 15 minutes post-bead beating resulted in a modest yield increase of 15%, but doubling the bead-beating time produced the highest-concentration extract with a 42% increase in DNA yield.

For the second experiment consisting only of physical modifications, increased intensity-time corresponded with a near-linear increase in total DNA concentration. Sonication for 30 minutes after bead beating produced similar results to sonication for 15

minutes, but increasing sonication time to an hour resulted in a 57% increase in DNA yield relative to the control sample, producing approximately the same effect as doubling the bead beating time in this experiment (60% increase in yield).

Because longer or more intense mechanical lysis during extraction may shear DNA, the quality of the extracted DNA was further assessed through digital electrophoresis. As expected, high-intensity lysis decreased the peak DNA fragment size in the extracts by up to 41% (intensity-time of 960 m) when compared against the control samples (intensity-time of 240 m) (Figure 2.3). This effect was much more pronounced for the sonicated samples, for which digital electrophoresis showed broad peaks corresponding to shorter DNA fragments, even for the shortest sonication time of 15 minutes (Table 2.1). The most intense bead beating modification did not exhibit nearly this much shearing, indicating that the trade-off between shearing and increased DNA yield is more relevant for sonication than for bead beating modifications.

Test 1: Chemical and physical modifications



Test 2: Physical modifications

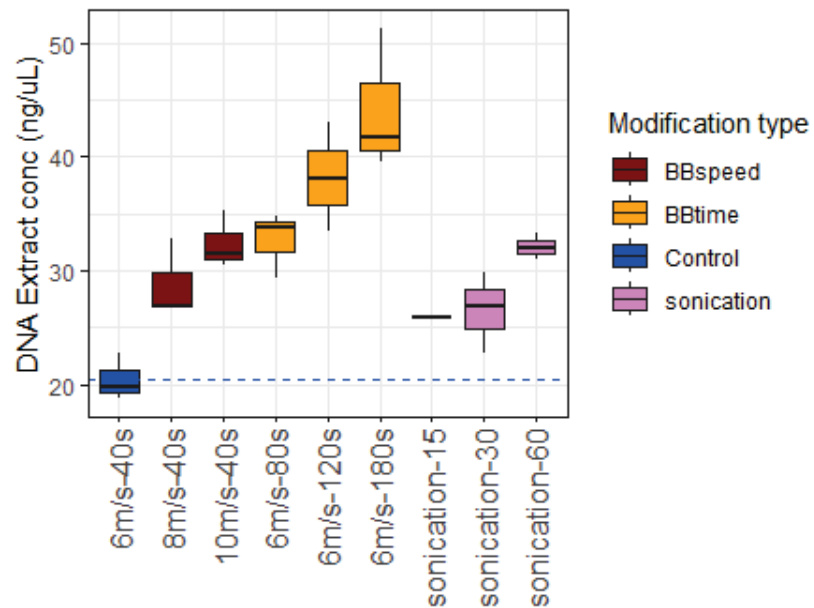


**Figure 2.2.** Final DNA concentrations of identical exhausted GAC samples extracted with different modifications to the Fast DNA Spin Kit for Soil protocol. Control samples (average concentration represented by blue horizontal lines) were extracted using the recommended kit protocol. Tested modifications included adjusting bead beating (BB) time, bead beating speed, sonication post-bead beating, and addition of chemical reagents to the provided kit extraction buffer. Reagents for the cell detachment solution (“Detach”) and skim milk powder (“MP”) were also directly extracted as controls for potential contamination.

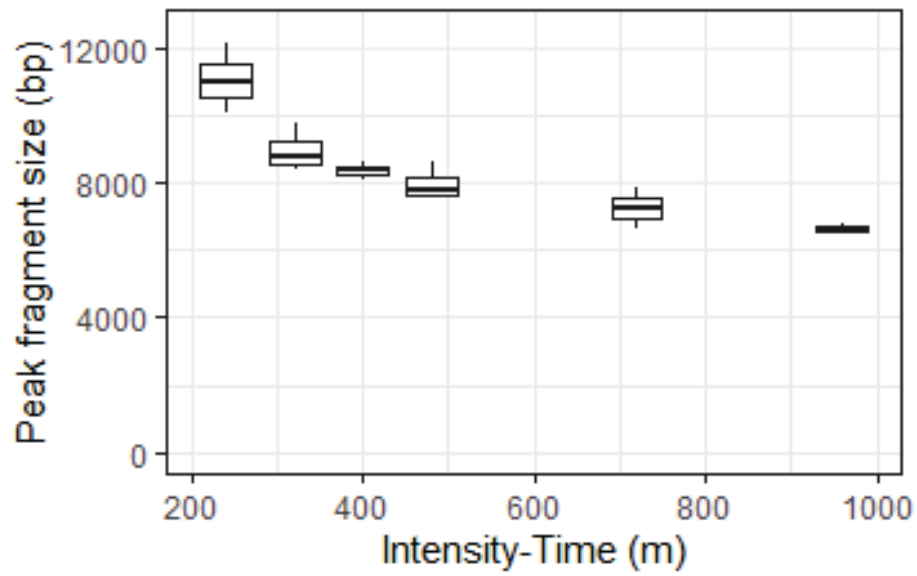
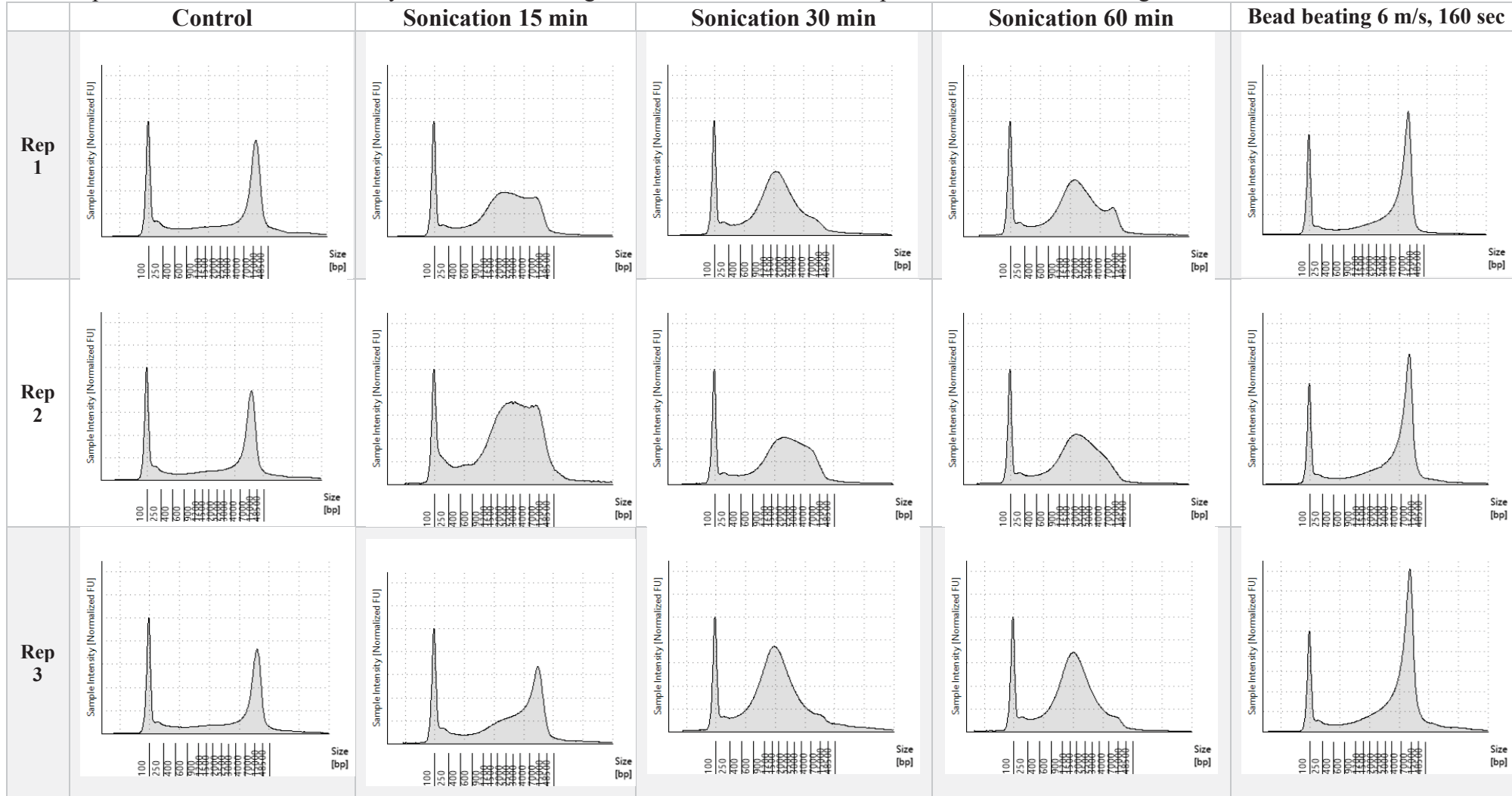


**Figure 2.3.** Peak DNA fragment sizes of extracts obtained from identical GAC samples extracted with various modifications to bead beating settings. Intensity-time represents the speed of bead beating times in meters per second times the duration in seconds.

**Table 2.1.** TapeStation traces of triplicate GAC extracts processed with different modifications. DNA fragment size is shown along the x-axis, y-axis values represent the fluorescent intensity of DNA at that fragment size. Peaks to the left represent low-molecular weight noise.



### 2.3.3 16S microbial community analysis

Phylum-level analysis of microbial samples collected from the top, middle, and bottom of an exhausted GAC contactor revealed a high degree of similarity between GAC-associated phyla at different strata (Figure 2.5). Proteobacteria was the dominant phylum in all collected samples, followed by Chloroflexi, Acidobacteria, and Planctomycetes. GAC collected from the lower portions of the contactor contained higher abundances of obligately anaerobic Chlorobi.

Visually, ordination plots of beta diversity clustered according to top versus middle/bottom GAC samples, with some arrangement according to increasing intensity-time (Figure 2.4). ADONIS tests on both weighted (Bray-Curtis) and unweighted (Jaccard) family-level beta diversity metrics revealed no significant effect of the extraction modification on microbial community composition, whereas the location of the GAC sample was significant. Post-hoc tests confirmed that only significant differences were found between the top and middle and the top and bottom GAC samples, while middle and bottom samples were highly similar in composition.

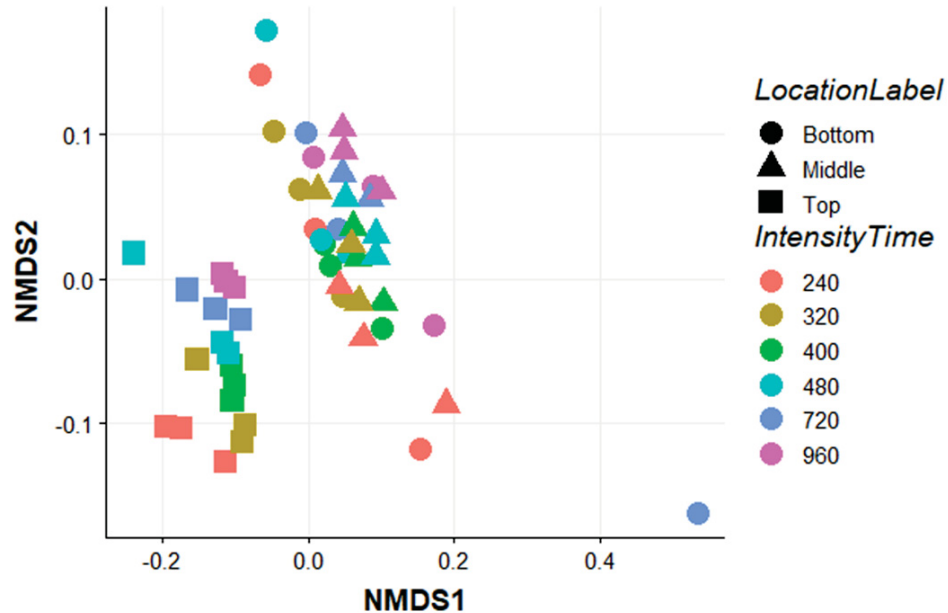


**Figure 2.4.** Bray-Curtis dissimilarity ordination plot comparing microbial community composition as determined from 16S rRNA gene sequencing of DNA recovered from GAC samples from the top, middle, and bottom of an exhausted contactor extracted with

indicated bead beating settings with variable speed/duration (Intensity-time representing the speed times the duration, where 240 is the control).

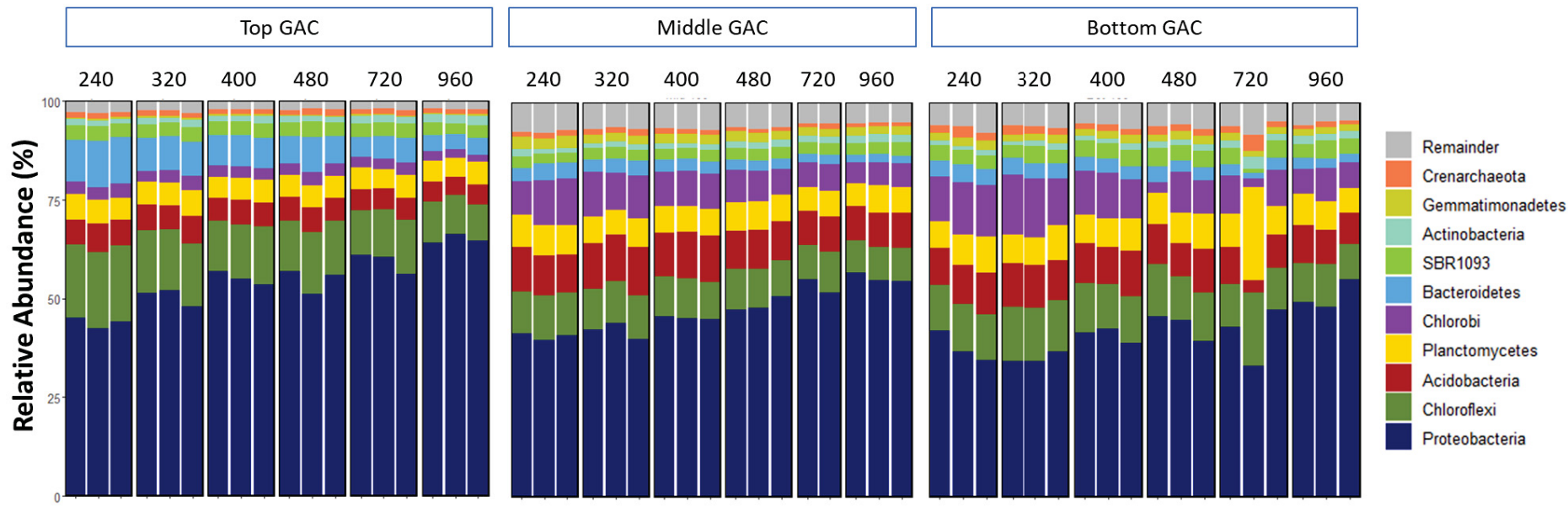


**Figure 2.5** Relative abundances of key GAC-associated phyla in triplicate samples collected from the top, middle, and bottom of an exhausted contactor and each extracted with six different bead beating settings. Numbers represent the intensity-time associated with each bead beating modification, where 240 is the control sample extracted according to the kit-recommended protocol.

## 2.4 Discussion

DNA was rapidly sorbed to virgin GAC, and sorption of over half of the original free DNA occurred after two hours of incubation. In the context of extraction, DNA released from bacterial cells via lysis may be exposed to GAC after bead beating for up to 20 minutes in this protocol (approximate time between the end of bead beating and the transfer of the DNA-containing supernatant to a clean, non-GAC containing tube). This result suggests that the main difficulties previously observed during extraction from exhausted GAC/BAC (Bacaro et al., 2019) may not be due to loss of the lysed DNA as a result of re-sorption to the media after bead beating, but rather due to strong attachment of cells/biofilms to the media.

While sorption showed promise for the use of GAC as a passive environmental sampler of extracellular DNA, results from extraction optimization tests on the DNA-exposed GAC highlight potential difficulties. Attempting to recover sorbed DNA from the virgin GAC after 24 hours of incubation was largely unsuccessful, recovering less than 10% of the expected concentration of sorbed DNA for all tested methods. Kirtane et al. (2020) previously reported similar results when attempting to extract DNA from 4 g of GAC exposed to 40 ng/ $\mu$ L extracellular DNA using four different commercial extraction kits, with yields consistently below 1%. In the same study, however, field trials of GAC samplers deployed in a stream for at least 7 days recovered comparable amounts of fish DNA to bulk water samples, indicating little difficulty in recovering sorbed DNA. This suggests that that GAC used as a passive sampler may be somewhat “exhausted” over a long (e.g., multi-day) exposure to environmental DNA, resulting in lower sorptive capacity and easier recovery of DNA.

Overall DNA extraction yields from exhausted GAC collected from a contactor in a potable reuse train demonstrated that addition of external chemical reagents (Denhardt’s solution or skim milk powder) to a commercial extraction kit did not increase yields as hypothesized. Detachment of cells using a detergent solution prior to extraction also appeared to be ineffective, again suggesting that strong attachment of biofilms complicates extraction. Yields were significantly increased through alteration of the mechanical lysis step, highlighting the importance of thorough physical disruption of strongly attached microbial communities during DNA extraction. Sonication for 60

minutes produced almost the same increase in DNA yield as doubling the bead beating duration (57% versus 60%). However, while DNA integrity was only moderately affected by increased bead beating, bath sonication resulted in much greater shearing of DNA. This points towards bead beating modification as the best approach for intensifying mechanical lysis of cells without sacrificing DNA quality. For shotgun sequencing approaches where DNA is fragmented prior to sequencing, the shearing observed here in non-sonicated samples is not extensive enough to warrant concern when modifying bead beating protocols, though long-read sequencing methods may be more sensitive to DNA length and integrity (Trigodet et al., 2022).

While increasing the intensity of mechanical lysis doubled yields, overall microbial community composition as determined through 16S rRNA sequencing was not significantly affected. Beta diversity statistics showed greater similarity of microbial communities based on location of the GAC sample within the contactor than on the sample processing method, indicating that modification of bead beating settings does not introduce significant bias to molecular community analysis in this application.

Additionally, community composition data collected in this experiment may help inform sampling of stratified GAC from contactors. Microbial communities within the “middle” portion of the GAC contactor were not differentiable from communities at the bottom of the contactor, but these were distinct from communities observed in GAC at the top of the contactor. Our sample collection methodology (collecting samples at different timepoints during emptying of the contactor) make this conclusion highly uncertain since we cannot be sure that the middle and bottom samples are truly stratified. However, these results are consistent with previous observations that GAC microbial communities change with depth due to nutrient and oxygen gradients, as seen here in the enrichment of anaerobic organisms in the middle and bottom GAC samples (Boon et al., 2011). Literature on stratified GAC microbial communities is scarce, but these findings suggest complexities in the microbial ecology of GAC biofilms in relation to contactor depth that may be worth further study.

## 2.5 Conclusion

This study found that strong attachment of biofilms to GAC is the primary challenge complicating extraction of microbial DNA from exhausted GAC and BAC. Increasing the intensity of mechanical lysis may resolve difficulties encountered in recovering microbial DNA from exhausted GAC and BAC, but the tendency of extracellular DNA to sorb to non-exhausted GAC remains a challenge, especially in the context of GAC as a passive environmental sampler. These findings are applicable to future studies on GAC/BAC microbial communities in a variety of water treatment systems, developments in the use of GAC as an environmental DNA sampler, and optimization of DNA extraction from other complex media aside from GAC, including other biofilter media types and environmental soils/sediments. Overall, we provide a thorough comparison of potential modifications to DNA extraction that may resolve previously encountered issues with extraction efficiency, providing guidance for future studies on microbial community dynamics within GAC and BAC.

## CHAPTER 3: Metagenomic Insights into Cometabolic Degradation of 1,4-Dioxane in Propane-Amended Biofilters for Water Reuse

### Abstract

Biostimulation with propane has been successfully applied for cometabolic biodegradation of 1,4-dioxane in groundwater and has more recently been applied to biofiltration for water reuse applications. Here we investigated the effect of propane amendment on microbial community composition and functional gene profiles of biologically-activated carbon (BAC) biofilters applied in a potable water reuse treatment train. BAC media and biofilter effluent samples were collected from duplicate control and propane-dosed biofilters over eight months of operation and were analyzed through shotgun metagenomic sequencing. Enhanced 1,4-dioxane removal in amended biofilters was associated with enrichment of *Mycobacteriaceae* and higher abundances of an operon containing two distinct soluble diiron monooxygenases (SDIMOs). Comparisons of microbial and chemical datasets suggested a five-week lag between initial establishment of SDIMO-harboring mycobacteria and observation of dioxane degradation activity. Loss of cometabolic 1,4-dioxane removal due to an operational disruption in propane feeding was reflected by only moderate decreases in abundances of *Mycobacteriaceae* and SDIMOs, and cometabolic activity was regained within two weeks of restart in one of the filters. Overall, specific microbial taxa and SDIMOs associated with cometabolic removal of 1,4-dioxane were enriched from native BAC microbial communities, and enriched communities demonstrated robust 1,4-dioxane removal capacity throughout fluctuating operational conditions.

### 3.1 Introduction

1,4-dioxane is a water-miscible, highly recalcitrant drinking water contaminant designated as a probable human carcinogen by the US Environmental Protection Agency (US EPA), with a one-in-one million cancer risk level of 0.35 µg/L in drinking water (US EPA, 2013). Considered a contaminant of emerging concern (CEC), it is not yet federally regulated despite a 2017 US EPA survey finding concentrations of 1,4-dioxane exceeding the health-based risk level in 7% of surveyed public drinking water distribution networks (Adamson et al., 2017). Due to its poor adsorption to granular activated carbon (GAC)

and the high cost of advanced oxidation processes for chemical degradation, there is a need to develop more effective and economical technologies for 1,4-dioxane removal (Godri Pollitt et al., 2019; Vatankhah et al., 2019). This need is particularly acute for potable reuse treatment trains, where compliance with health-based contaminant limits is vital to ensure that public health is adequately protected. If proved effective, biological removal of 1,4-dioxane is an attractive alternative treatment method that could provide more extensive degradation at a lower cost than current technologies.

Biodegradation of 1,4-dioxane has historically been studied in the context of groundwater remediation. Several bacterial strains have been identified that can directly metabolize mg/L levels of dioxane, but the very low concentrations of 1,4-dioxane typically encountered in the field tend to be insufficient to support growth of dioxane metabolizers (Barajas-Rodriguez & Freedman, 2018; Inoue et al., 2016; Zenker et al., 2004). This limitation can be successfully overcome through cometabolic stimulation of native groundwater and soil microorganisms with primary substrates including simple alkane or alkene gases (e.g. propane, ethane, ethene) and cyclic and/or aromatic compounds (e.g. tetrahydrofuran, toluene) (Xiong et al., 2020). A recent pilot-scale study demonstrated that cometabolic degradation of  $\mu\text{g/L}$  level 1,4-dioxane could be achieved through amending n-butane upstream of a drinking water biofilter (McElroy et al., 2023). In another recent study, also at  $\mu\text{g/L}$  influent levels of 1,4-dioxane, biological removal was achieved in a potable reuse train through propane or tetrahydrofuran addition (Stohr et al., 2023). Of these co-substrates, propane has been widely applied in many environmental remediation applications due to its nontoxicity, wide availability, and low cost (Bell et al., 2022; Lippincott, 2015).

Biodegradation of 1,4-dioxane cometabolically or as a growth substrate has been attributed to the activity of aerobic bacteria harboring diverse alkane-, alkene-, and aromatic-oxidizing soluble diiron monooxygenases (SDIMOs). SDIMOs are multicomponent enzymes organized into six subgroups based on the structural similarity of their alpha subunit, their operon structure, and their substrate preference (Table 1) (Coleman et al., 2006; Leahy et al., 2003; Notomista et al., 2003). SDIMOs have been identified among a wide distribution of Gram positive and Gram negative bacterial taxa, mainly within the phyla Actinobacteria and Proteobacteria. SDIMO-encoding genes are

correspondingly thought to be horizontally exchanged through mobile genetic elements (Goff & Hug, 2022). In particular, the genera *Mycobacterium*, *Rhodococcus*, and *Pseudonocardia* are highly represented in SDIMO literature (D. Deng et al., 2018; Inoue et al., 2016; Masuda et al., 2012).

Characterization of bacterial communities associated with cometabolic dioxane degradation has largely been limited to general taxonomic analysis and quantitative measurement of known SDIMO genes using published SDIMO primer sets (He et al., 2018; Inoue et al., 2020). Few studies have attempted to explore SDIMO gene diversity in environmental samples. Such studies have typically relied on polymerase-chain reaction (PCR)-based methods (Coleman et al., 2006; Holmes & Coleman, 2008; M. Li et al., 2013), which introduce primer bias and cannot be guaranteed to capture the full diversity of SDIMOs in a given sample. Metagenomic sequencing of 1,4-dioxane-cometabolizing communities has been proposed as a way of identifying novel genes, microorganisms, and pathways involved in 1,4-dioxane biodegradation (S. Zhang et al., 2017).

The objective of this study was to expand upon knowledge of the diversity of SDIMOs and microbial taxa involved in cometabolic biodegradation of 1,4-dioxane through metagenomic analysis of potable reuse BAC biofilters that successfully degrade 1,4-dioxane at trace ( $\mu\text{g/L}$ ) levels. Concurrent chemical and microbiological data were collected from propane-amended and control biofilters to compare microbial signatures associated with enhanced dioxane removal. We specifically aimed to identify key taxa and SDIMOs likely involved in 1,4-dioxane degradation, to determine the diversity and abundance of native versus propane-enriched SDIMOs in typical BAC biofilters, and to capture microbial community shifts associated with changes in biofilter operation and performance.

**Table 3.1.** Overview of SDIMO subfamilies as designated by Holmes and Coleman (2008). Arrangements of genes coding for  $\alpha$ ,  $\beta$ ,  $\gamma$  subunits, Reductase (R) and Effector (E) proteins, and additional group-specific features in the SDIMO operon are indicated.

<b>SDIMO GROUP</b>	<b>PRIMARY TARGET</b>	<b>FREQUENTLY ASSOCIATED SUBSTRATES</b>	<b>OPERON STRUCTURE</b>	<b>UNIQUE OPERON COMPONENTS</b>	<b>EXAMPLES</b>
<b>GROUP 1</b>	Aromatics	toluene, propene, benzene	$\alpha$ - $\gamma$ -Ferro-E- $\beta$ -R	Rieske-type ferredoxin	<i>Pseudomonas mendocina</i> KR1 Tmo
<b>GROUP 2</b>	Aromatics	phenol, substituted aromatics	Fp- $\beta$ -E- $\alpha$ - $\gamma$ -R	Fp putative complex assembly peptide	<i>Pseudomonas sp.</i> CF600 Dmp, <i>Burkholderia cepacia</i> G4 Tom
<b>GROUP 3</b>	Aliphatics	methane, butane	$\alpha$ - $\beta$ -E- $\gamma$ -orfY-R	orfY immediately upstream (function unknown)	<i>Methylosinus trichosporium</i> OB3b mmoX
<b>GROUP 4</b>	Aliphatics	ethene, propene, alkenes	$\beta$ -E- $\alpha$ -R		<i>Rhodococcus corallinus</i> B-276 Amo
<b>GROUP 5</b>	Aliphatics	propane, THF	$\alpha$ -R- $\beta$ -E		<i>Pseudonocardia sp.</i> K1 thm, <i>Rhodobacter sphaeroides</i> 2.4.1
<b>GROUP 6</b>	Aliphatics	propane	$\alpha$ - $\beta$ -E-R		<i>Gordonia sp.</i> TY-6 Prm, <i>Mycobacterium</i> NBB4

## 3.2 Methods

### **3.2.1 Experimental design and sampling**

The experimental setup consisted of four BAC biofilters operated in parallel since 2019 in a 1 MGD potable reuse facility receiving secondary effluent from a 5-stage Bardenpho wastewater treatment plant (Hampton Roads Sanitation District SWIFT Research Center, Suffolk, VA). Further details concerning upstream treatment and biofilter construction and operation are provided in Supplemental Text 3.1. Background sampling of effluent from all biofilters was conducted prior to the start of cosubstrate addition in June 2022, when propane amendment was initiated in two of the biofilters (PROPANE-1 and PROPANE-2) through an in-line mixer (Figure 3.1A). Bulk water samples were collected weekly over a period of 8 months for monitoring of influent and effluent concentrations of 1,4-dioxane and propane through GC/MS (EPA Method 522, Eurofins). Target propane doses ranged from 2 to 8 mg/L over the course of the study, though volatility and difficulty in dissolution of the dissolved propane resulted in actual transferred doses ranging from 1 to 6 mg/L as determined through influent GC/MS measurements. Biofilters were periodically backwashed according to turbidity, head loss accumulation, and run time thresholds (Supplemental Text 3.1). PROPANE-1 and CTRL-1 were additionally dosed with 0.05 mg/L-P phosphoric acid to examine the role of phosphorus as a possible limiting nutrient in TOC and/or contaminant removal.

At each microbial sampling event, triplicate 1L effluent samples from all four biofilters were collected in autoclaved polypropylene Nalgene bottles. Field and trip blanks consisting of autoclaved MilliQ water were also included for every sampling event. Following observation of enhanced 1,4-dioxane removal in August of 2022, BAC media grab samples were also collected in sterile 50 mL Falcon tubes from the top of each biofilter using an ethanol-sterilized scoop. Biofilter effluent (hereon designated “Effluent”) and media (hereon designated “BAC”) samples were shipped overnight on ice to Virginia Tech and were processed within 24 hours of collection. Effluent samples were vacuum-concentrated onto 0.22  $\mu\text{m}$  mixed cellulose ester filters (S-Pak, Millipore Sigma). Filters were torn into uniform pieces with sterilized forceps and transferred to extraction tubes. BAC samples were freeze-dried overnight at  $-84^{\circ}\text{C}$  (Labconco FreeZone) and aseptically transferred into triplicate extraction tubes in 200 mg aliquots

(dry weight). All samples were stored at -20°C prior to extraction using the Fast DNA Spin Kit for Soil (MP Bio) following manufacturer protocol, with a slight modification to the bead-beating step for BAC samples (8 m/s for 80s rather than 6 m/s for 40s).

### **3.2.2 Shotgun metagenomic sequencing**

A total of 94 DNA extracts from BAC media, effluent, and blank samples were quantified using the Qubit High Sensitivity dsDNA assay kit. BAC extracts were diluted 1:10 prior to preparation for sequencing due to high DNA concentration and potential presence of media-derived inhibitors. Triplicate extracts were pooled at equal mass and processed at the Duke Genomic Sequencing Core for library preparation and 150 bp paired-end sequencing on two full Illumina NovaSeq 6000 S4 flow cells. Per-sample read depths ranged from 40-140 million reads, with an average quality score of 35.4 for the two flow cells.

### **3.2.3 Bioinformatic analysis**

Raw forward and reverse reads were concatenated across flow cell lanes and quality filtered with fastp (S. Chen et al., 2018). Contaminant sequences (i.e. human, cat, dog, and rodent DNA) were removed with bbdduk (minlength = 51) (Bushnell, 2014). Reads passing QA/QC were then assembled *de novo* with MegaHIT, and PRODIGAL was used for ORF and protein prediction from assembled contigs (Hyatt et al., 2010; D. Li et al., 2015). Taxonomic data was extracted from QCed reads using kraken2 and bracken for relative abundance estimation using a database constructed from the default bacterial and archaeal libraries (J. Lu et al., 2017; J. Lu & Salzberg, 2020). Differential abundance analysis was performed with DESeq2 in R at the genus level to identify taxa significantly enriched in the propane-amended biofilters compared to control biofilters after observation of enhanced 1,4-dioxane removal (Love et al., 2014).

Functional gene analysis was conducted using a manually-curated database of SDIMO alpha subunit sequences representing all 6 subgroups constructed through literature review and querying of the UniProt database for propane, tetrahydrofuran, toluene, methane, ethene, phenol, and benzene monooxygenases and hydroxylases (Supplemental Table 3.1) (The UniProt Consortium, 2023). Alpha subunit sequences were selected because they are the most conserved components of SDIMOs and contain

unique signatures within subgroups (Leahy et al., 2003). The resulting 45 sequences were aligned in Geneious and organized into a phylogeny using the Geneious tree builder (Geneious Prime 2023.2). PRODIGAL-predicted protein sequences from all media samples were queried against the curated SDIMO protein database using DIAMOND blastp with the “very-sensitive” setting (max-target-seqs = 1, minimum subject cover of 50%) (Buchfink et al., 2015). Aligned query sequences were imported into Geneious and annotated with the conserved SDIMO motifs listed in Supplemental Table 3.2. Some sequences contained few (< 3) or none of the conserved motifs, indicating likely false positives in the blastp output. Sequences were therefore filtered to retain only those hits which contained at least four occurrences of the motifs, and these sequences were compiled to generate a list of putative SDIMOs. This compiled list was then clustered at 100% amino acid sequence identity to dereplicate identical SDIMO alpha subunits using CD-HIT (Fu et al., 2012).

For relative quantification, quality-filtered forward reads were mapped to these putative SDIMO alpha subunit sequences using DIAMOND blastx with an identity criterion of 100% (max-target-seqs = 1). The two topmost abundant SDIMOs were queried against the NCBI non-redundant database. Contigs generated from MegaHIT containing the topmost abundant SDIMO alpha subunit sequences were analyzed through operon-mapper to identify the putative genes surrounding these alpha subunit sequences and to reveal the organization of the putative SDIMO operon for confirmation of subgroup classification (Taboada et al., 2018).

All statistical analysis was conducted in RStudio. Diversity matrices were generated from bracken feature tables using the vegan package (Oksanen et al., 2022). ANOSIM tests were conducted using a cutoff p-value of 0.05.

### 3.3 Results

#### **3.3.1 Enhanced 1,4-dioxane removal in propane-dosed biofilters**

Influent 1,4-dioxane concentrations over the course of the study ranged from 0.15 to 0.37 µg/L. Figure 1 provides a timeline of biofilter operational changes and chemical monitoring data throughout the course of microbial sampling. After one month of propane amendment, a DO drop was observed that indicated seeding of the amended

biofilters with a propane-enriched microbial community. Enhanced removal of 1,4-dioxane in PROPANE-1 and PROPANE-2 relative to the control filters (> 50% difference in removal rates) was first observed approximately two months after the start of amendment in August 2022. This apparent cometabolic dioxane degradation was maintained for about two months until November 2022, when a malfunction in the in-line mixer resulted in a nine week pause in propane amendment during which chemical and microbial samples were not collected. Immediately prior to the restart of propane amendment in January 2023, a second set of background microbial samples was collected, followed by two additional weekly samplings to monitor the recovery of cometabolizing microbial communities as propane was reintroduced. Chemical data indicated that enhanced removal of 1,4-dioxane in PROPANE-1 and PROPANE-2 was lost over the course of the interruption, but PROPANE-1 exhibited enhanced removal (83%) as soon as two weeks after addition of propane was recommenced. PROPANE-2 experienced only a slight increase in removal at this time (39% removal two weeks post-restart versus 11% removal during the recovery phase).

From these trends in the chemical data, we designated four main experimental phases: the background phase from June to late August during which cometabolic dioxane removal was not observable, the cometabolic phase from August to October during which apparent cometabolic activity was consistently removing dioxane in the propane-amended biofilters, the recovery phase after January during which biofilter communities experienced a second acclimation period after propane was reintroduced, and the final post-recovery sampling event where only one filter appeared to fully regain cometabolic activity. Figure 3.2 illustrates the clear differences in dioxane removal between these phases. TOC removal rates were consistent between all four biofilters throughout the experiment and generally ranged between 20-30% (Supplemental Figure 3.1).

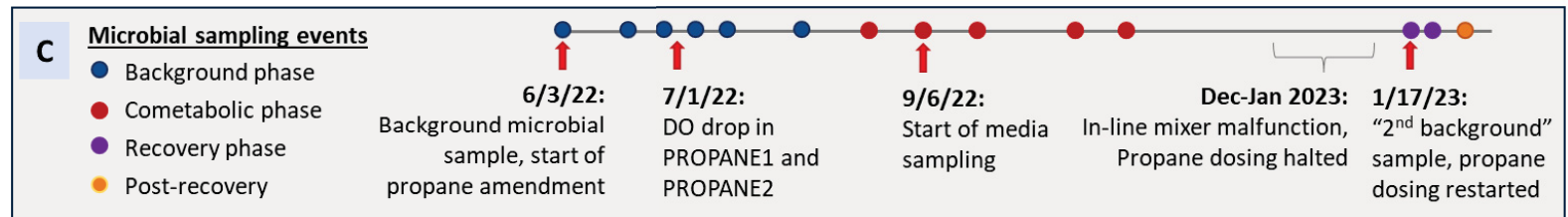
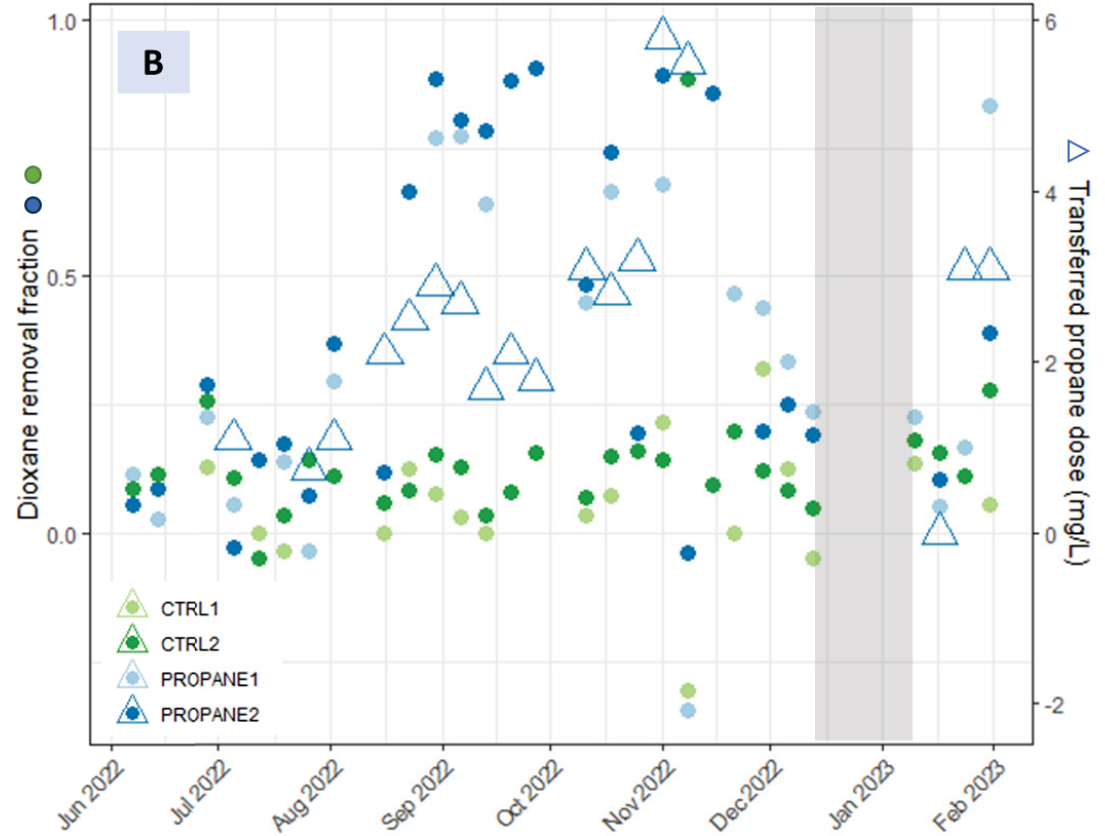
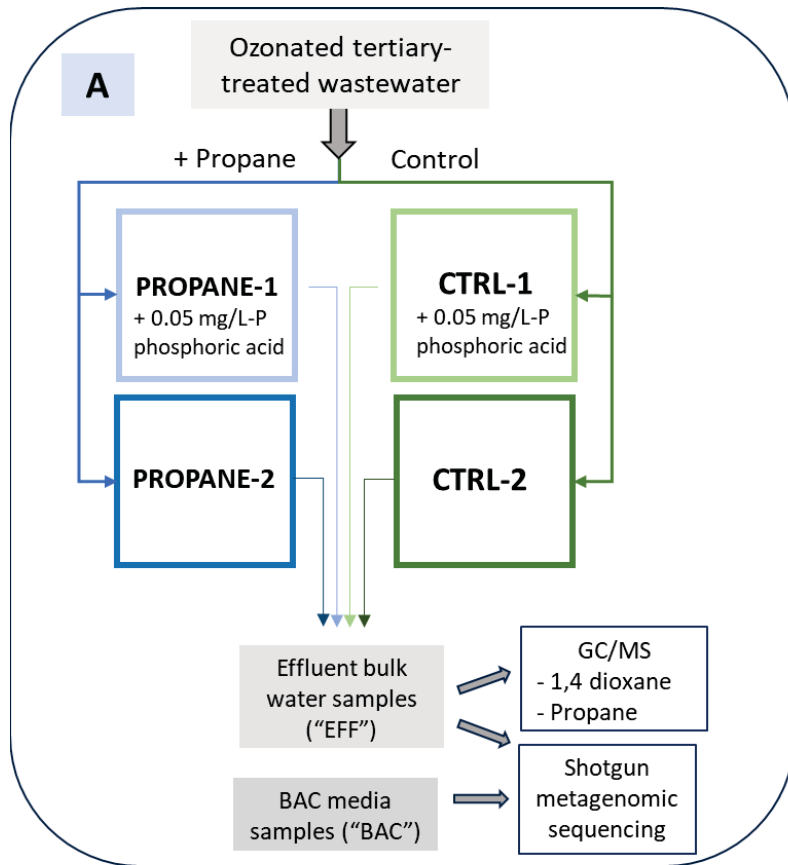


**Figure 3.1** **A)** Schematic of biofilter experimental setup. Influent ozonated tertiary-treated wastewater was split into propane-amended and control lines, each feeding two full-scale BAC biofilters. One control and one propane-amended biofilter also received 0.05 mg/L-P phosphoric acid. Effluent bulk water samples were processed for both chemical and microbial analysis, and BAC media samples collected from the top of all four filters were processed for microbial analysis starting on 9/6/22. **B)** GC/MS-determined 1,4-dioxane removal fraction in all four biofilters (left axis, colored circles) and transferred propane dose in propane-amended filters PROPANE-1 and PROPANE-2 (right axis, empty triangles) over the course of the study. An in-line mixer malfunction during which propane amendment was halted is highlighted in gray. **C)** Timeline of microbial sampling events relative to the above chemical sampling events, with key operational changes and observations noted. Microbial sampling events were categorized into four phases based on observed trends in 1,4-dioxane removal in PROPANE-1 and PROPANE-2: a background phase during which 1,4-dioxane removal was comparable between propane-amended and control filters, a cometabolic phase during which 1,4-dioxane removal in the propane-amended filters was significantly higher than removal in the control filters, a recovery phase during which propane amendment was restarted after the two-month operational disruption which resulted in an apparent loss of cometabolic activity, and a single post-recovery event in which cometabolic activity was apparently recovered in only one of the propane-amended biofilters.

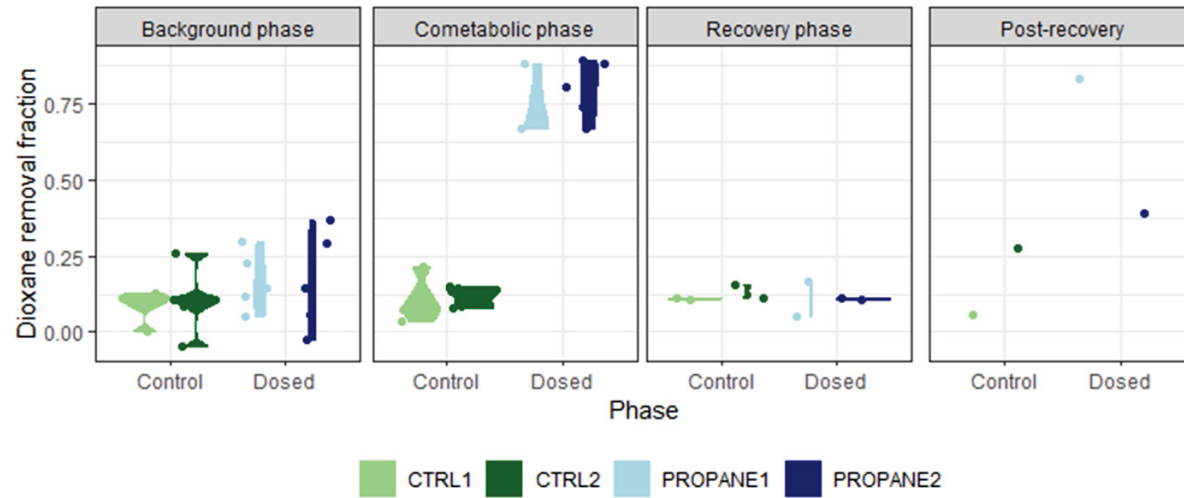


**Figure 3.2.** Violin plots of 1,4-dioxane removal fractions averaged across sampling events within each experimental “phase” as defined by apparent activity of cometabolizers within the propane-dosed biofilters.

### 3.3.2 Microbial community shifts in response to propane amendment

Visually, clusters in a Bray-Curtis NMDS plot of BAC media communities displayed clear separation between the three experimental phases (Figure 3.3). Family-level Bray-Curtis ANOSIM tests on samples taken during the cometabolic phase confirmed significant differences in the microbial community compositions of BAC media from propane-dosed versus control biofilters ( $R = 0.84$ ), though this difference was not significant ( $p > 0.05$ ) in effluent samples. Additionally, BAC communities from amended biofilters showed significant differences when comparing samples before the disruption event versus after ( $R = 0.93$ ). DESeq2 analysis at the genus level revealed significant enrichment of the genera *Mycobacterium* and *Mycolicibacterium* in propane-dosed versus control filters (Figure 3.4) (Wald statistic = 99 for *Mycolicibacterium* and 67 for *Mycobacterium*). Other enriched genera included *Nocardia*, *Gordonia*, *Mycolicibacillus*, and *Cellulosimicrobium*; however, these genera were present at much lower relative abundances (0.0001-0.001) compared to *Mycobacterium* and *Mycolicibacterium* (up to 0.1). Effluent samples taken approximately five weeks before observation of enhanced dioxane removal show a sudden spike in the relative abundance of *Mycobacterium* and *Mycolicibacterium* by nearly an order of magnitude (Figure 3.5). Relative abundances of these two genera were significantly lower in samples taken after the propane interruption event, though they were still highly enriched in dosed media compared to control filter media samples (Figure 3.5).

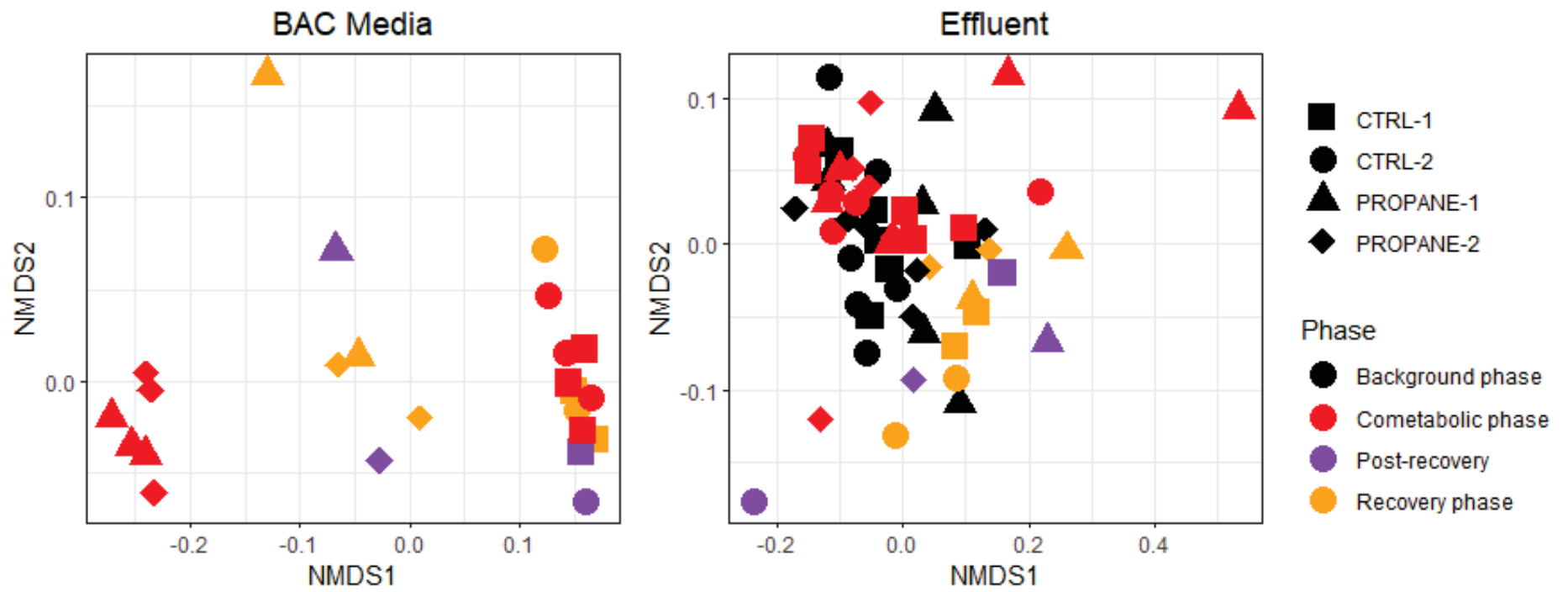


**Figure 3.3.** NMDS plots representing Bray-Curtis dissimilarity of all BAC media and effluent samples. Samples are colored according to experimental phase.

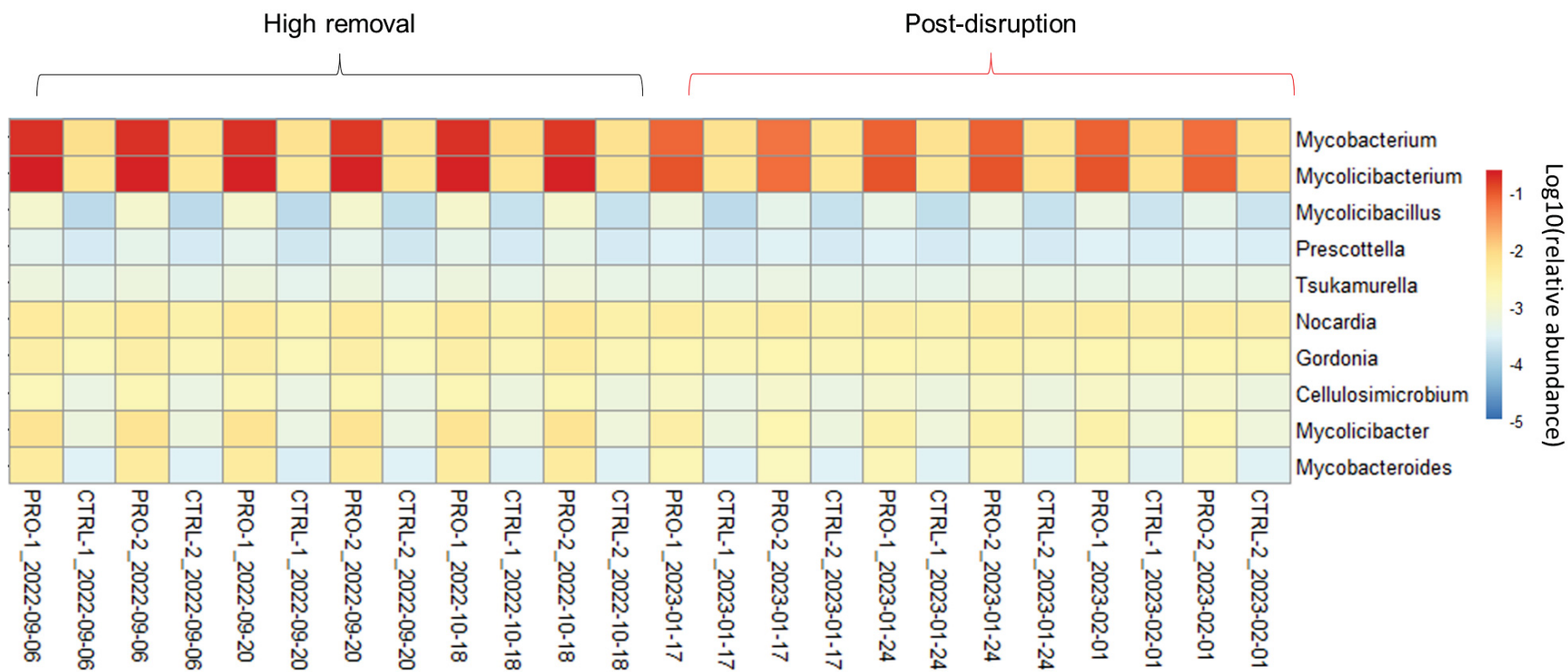


**Figure 3.4.** Heatmap of the 10 most significantly propane-enriched (highest Wald statistic) genera as determined through DESeq2 comparison of propane-dosed and control biofilter media (BAC). Heatmap colors represent the log relative abundances of each genus in each media sample (red = more abundant, blue = less abundant). X-axis labels show the sampling event and biofilter ID.

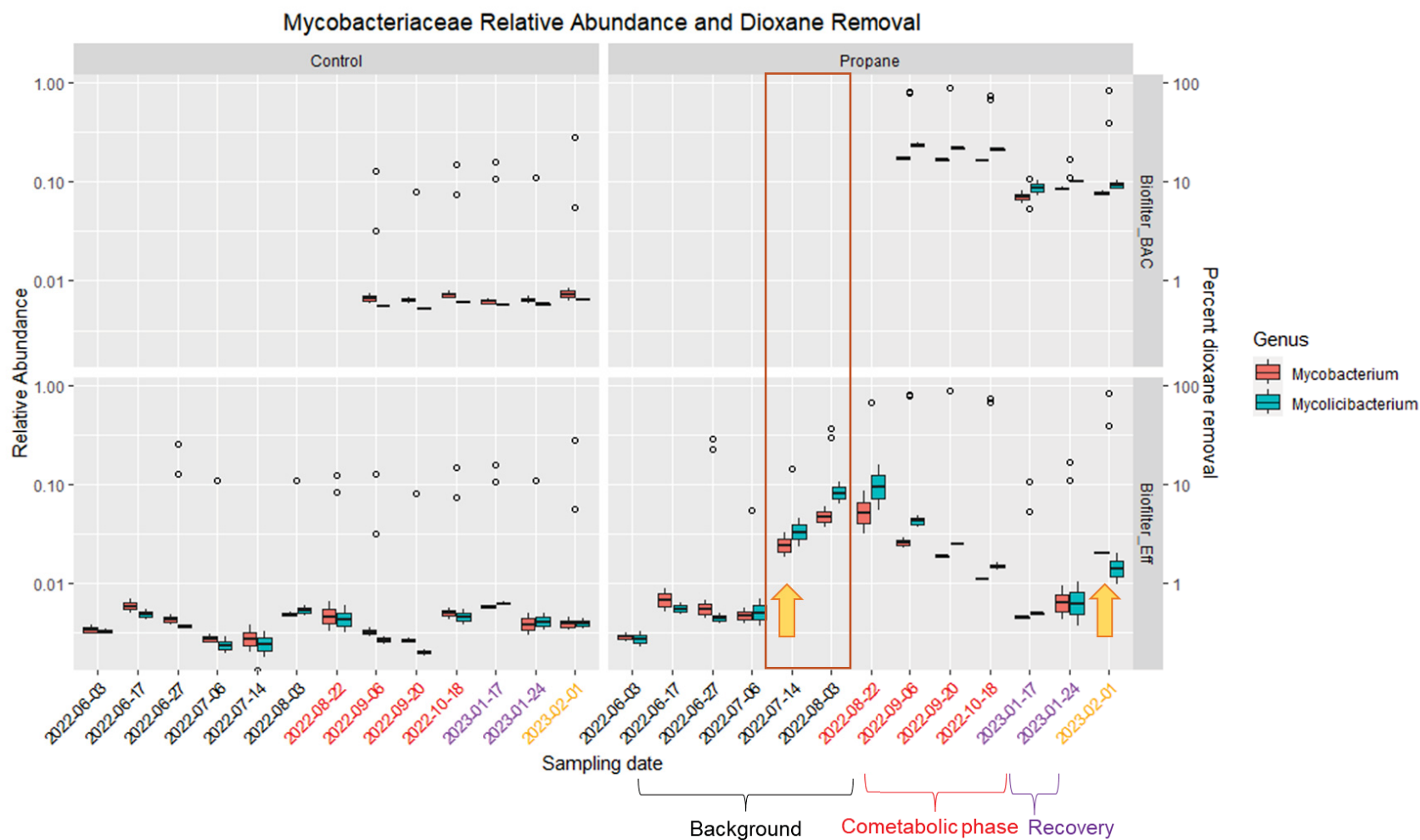


**Figure 3.5.** Log relative abundances of *Mycobacterium* and *Mycolicibacterium* in BAC (top) and biofilter effluent (bottom) from propane-dosed and control filters, averaged across duplicates. Percent dioxane removal is plotted on the right axis in open circles. A potential lag period in activation of dioxane cometabolism is highlighted in the orange box. Two orange arrows indicate periods of rapid growth and colonization concurrent with increases in dioxane removal. Sampling dates are colored by experimental phase.

### 3.3.3 Quantity and diversity of SDIMO genes in bulk water and BAC media samples

623 unique (clustered at 100% amino acid identity) putative SDIMO alpha subunit sequences were identified across the 28 media samples. These sequences were aligned and placed into a phylogeny with the 45 database sequences to determine their most closely related SDIMO subgroup through alpha subunit sequence homology. The annotated BAC-derived sequences represented SDIMOs from all six subgroups, with the highest number of unique sequences from Group 1 (propane and toluene monooxygenases).

Richness of SDIMOs was compared between dosed and control biofilter media and effluent over time. Effluent samples contained an estimated two to three times fewer unique SDIMOs when compared to respective media samples. SDIMO richness was consistently higher in propane-dosed media and effluent samples compared to control samples during the cometabolic phase. However, control samples still harbored diverse SDIMOs throughout the course of the study despite the absence of propane, though most of these sequences were limited to groups 1, 2, and 5.

SDIMO hit counts from blastx were normalized by total read counts and summed within their respective subgroups to determine the total reads per kilobase million (RPKM) for each of the six SDIMO subgroups (Figure 3.6). Total abundance of all putative SDIMOs was significantly higher in the cometabolic-phase dosed media than in the recovery phase media and undosed media. One week after reinitiation of propane amendment, total SDIMO abundance in PROPANE-1 media increased to near pre-starvation levels (90.1 RPM versus an average of 100 RPM prior to starvation) while PROPANE-2 SDIMO abundances remained relatively low. Effluent samples showed similar trends in total SDIMO abundance, though diversity of SDIMOs in effluent samples was not representative of the diversity found in media (Figure 3.7). Similar to trends in *Mycobacteriaceae*, SDIMO abundance in effluent spiked weeks before the first data point showing significantly enhanced removal of 1,4-dioxane (three week lag in PROPANE-1, five week lag in PROPANE-2).

Two putative SDIMOs (see Figure 3.6, labeled Put. G1 and Put. G2) were highly enriched in biofilter media, making up the majority of reads for SDIMO groups 1 and 2. Both of these SDIMO-like sequences were derived from the same contig, indicating that these genes belonged to the same operon or adjacent operons within the same organism. A significant linear correlation was found between the combined abundances of these two SDIMOs and the

combined relative abundances of *Mycobacterium* and *Mycolicibacterium*, suggesting that these SDIMOs were specifically associated with at least one of these genera (Figure S1, Adjusted  $R^2 = 0.90$ ,  $p$ -value  $< 0.001$ ).

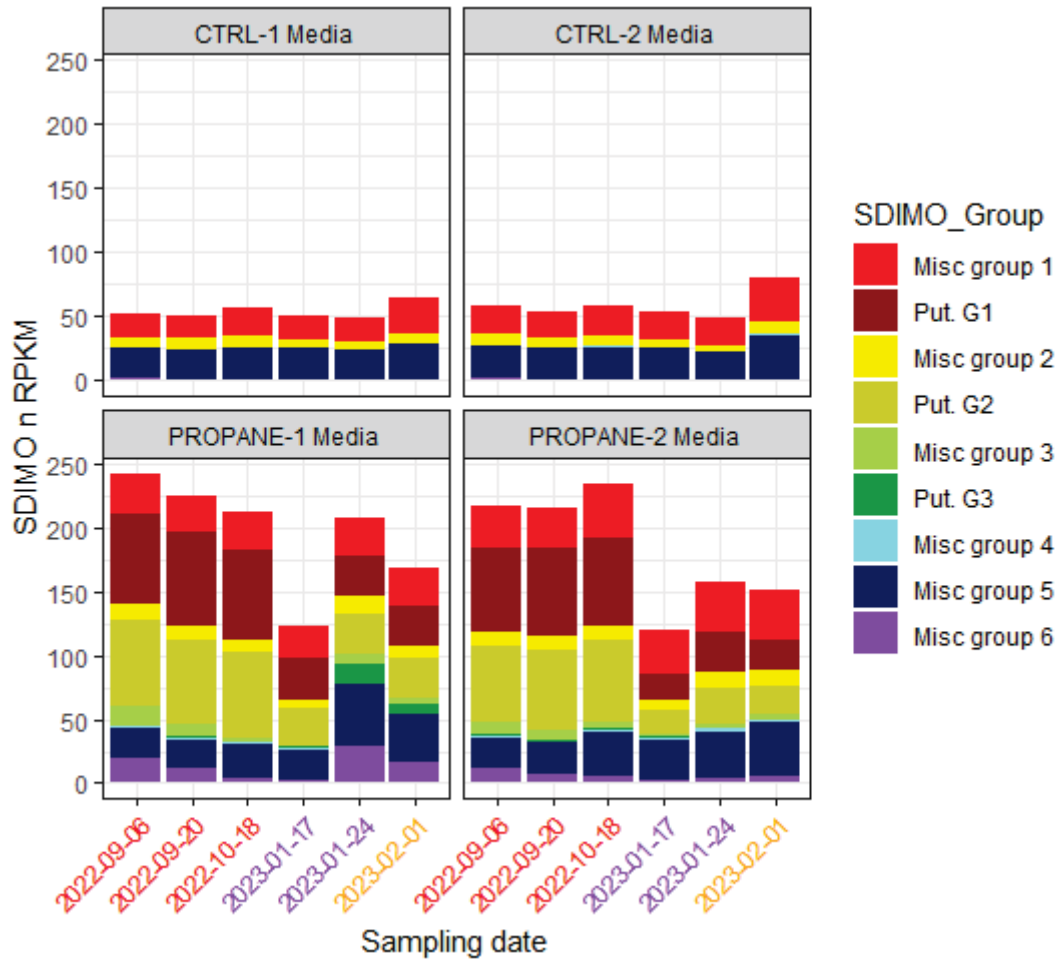


**Figure 3.6** Estimated abundances of the six SDIMO subgroups (“Misc.”) and three specific putative SDIMOs in BAC samples. Sampling dates are colored according to experimental phase (red = cometabolic phase, purple = recovery phase, orange = post-recovery).

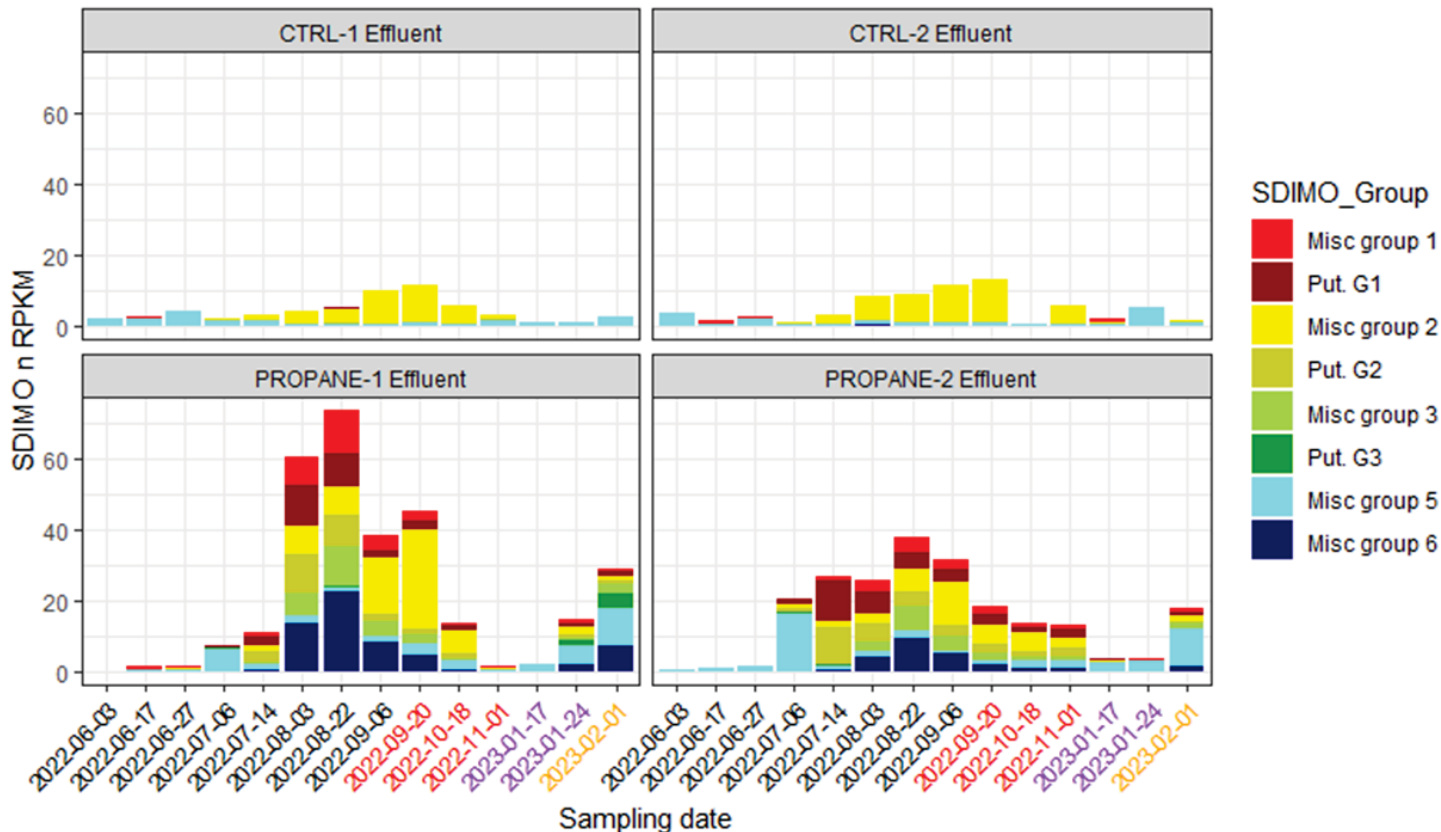


**Figure 3.7** Estimated abundances of the six SDIMO subgroups (“Misc.”) and three specific putative SDIMOs in biofilter effluent samples. Sampling dates are colored according to experimental phase (black = background phase, red = cometabolic phase, purple = recovery phase, orange = post-recovery).

When queried against the non-redundant protein sequences database through blastp, the highly abundant putative G1 and G2 SDIMOs returned best hits for putative aromatic monooxygenases or YHS-domain-containing proteins from *Mycobacterium helveticum* and *Amycolatopsis acidiphila* (~80% identity, Tables 3.2 and 3.3). Characterization of their surrounding operon components using operon-mapper confirmed that these were complete SDIMO operons belonging to groups 1 and 2 (Table 3.4). The group 1 toluene monooxygenase-like putative SDIMO was found to be spatially associated with three genes potentially involved in the breakdown of intermediates generated during toluene metabolism.

**Table 3.2** Blastp hits for the Group 1-like putative SDIMO alpha subunit.

Query ID	Subject Description	Organism	Subject Accession	Percent Identity	Score
k141_1353824_30	YHS-domain-containing protein	<i>Mycobacterium helveticum</i>	WP_144950954.1	85.827	939
k141_1353824_30	YHS-domain-containing protein	<i>Amycolatopsis acidiphila</i>	WP_144639178.1	87.033	931
k141_1353824_30	YHS-domain-containing protein	<i>Carbonactinospora thermoautotrophica</i>	WP_067071285.1	82.711	902
k141_1353824_30	YHS-domain-containing protein	<i>Carbonactinospora thermoautotrophica</i>	WP_066883940.1	82.711	902
k141_1353824_30	YHS-domain-containing protein	<i>Carbonactinospora thermoautotrophica</i>	WP_267594094.1	82.318	900

**Table 3.3** Blastp hits for the Group 2-like putative SDIMO alpha subunit.

Query ID	Subject Description	Organism	Subject Accession	Percent Identity	Score
k141_1353824_25	aromatic/alkene/methane monooxygenase hydroxylase/oxygenase subunit alpha	<i>Mycobacterium helveticum</i>	WP_144950948.1	83.135	905
k141_1353824_25	YHS domain-containing protein	<i>Amycolatopsis acidiphila</i>	TVT21728.1	83.333	904
k141_1353824_25	toluene monooxygenase	<i>Streptomyces liliiviolaceus</i>	WP_210893699.1	82.02	881
k141_1353824_25	aromatic/alkene/methane monooxygenase hydroxylase/oxygenase subunit alpha	<i>Amycolatopsis acidiphila</i>	WP_229858581.1	83.436	879
k141_1353824_25	toluene monooxygenase	<i>Streptomyces tauricus</i>	WP_265647490.1	82.222	878

**Table 3.4** Putative degradation genes associated with the two most abundant SDIMO-like sequences in the propane-amended biofilters. Both putative SDIMOs were found on the same contig (total contig length = 31,398 bp). Orders of the SDIMO component genes within each operon confirmed that the two putative SDIMOs belonged to subgroups 1 and 2 (see Table 3.1), as predicted through alpha subunit sequence homology. The toluene monooxygenase-like operon was associated with an operon containing three additional genes potentially playing a role in the catabolism of toluene degradation intermediates.

Operon	Putative gene	Start position	End position	Length (bp)	Sense
Putative Group 2 SDIMO (phenol hydroxylase) <b>Fp-β-E-α-γ-R</b>	dmpP (Reductase)	26311	27366	1056	reverse
	dmpO (Gamma)	27436	27771	336	reverse
	dmpN (Alpha)	27776	29305	1530	reverse
	dmpM (Effector)	29318	29608	291	reverse
	dmpL (Beta)	29605	30612	1008	reverse
Putative Group 1 SDIMO (toluene monooxygenase) <b>α-γ-Ferro-E-β-R</b>	Dioxygenase-like Reductase	20669	21511	843	reverse
	tmoE (Beta)	21660	22670	1011	reverse
	tmoD (Effector)	22674	22982	309	reverse
	tmoC (Ferredoxin)	22993	23364	372	reverse
	tmoB (Gamma)	23361	23606	246	reverse
	tmoA (Alpha)	23637	25151	1515	reverse
Accessory catabolism genes found in aerobic toluene degradation pathway	Transcriptional regulator	25419	26183	765	reverse
	2-oxopent-4-enoate hydratase	16363	17136	774	forward
	Acetaldehyde dehydrogenase	17162	18148	987	forward
	4-hydroxy-2-oxovalerate aldolase	18145	19167	1023	forward

### 3.4 Discussion

#### **3.4.1 Mycobacteria**

Propane biostimulation of native BAC microbial communities was effective in enhancing 1,4-dioxane degradation through the enrichment of dioxane-cometabolizing bacteria.

*Mycobacterium* and *Mycolicibacterium* were identified as the most enriched and most abundant genera in the propane-amended filters compared to the control filters. Relative abundances of these two taxa differed between control and dosed media by an order of magnitude, and together they represented up to an overwhelming 42% of the total propane-amended BAC microbial community during periods of high dioxane removal. Influent doses of propane ranged from 1 to 6 ppm while influent total organic carbon influent levels generally remained between 6 and 8 ppm (Supplemental Figure 3.1). Propane therefore represented a substantial proportion of influent TOC, providing an explanation for why biomass was so drastically impacted by amendment.

Relative abundances of *Mycobacterium* and *Mycolicibacterium* strongly correlated with abundances of the putative group 1 and group 2 SDIMOs, which were found on the same contig and therefore likely reside in the same organism (Figure S1). This (combined with their high sequence similarities to a *Mycobacterium* species as determined through BLAST) strongly implicates a member of the family *Mycobacteriaceae* as the principal cometabolizer of dioxane in this system and the host of the operon(s) containing the two key putative SDIMOs, in agreement with previous studies which have identified environmental *Mycobacteriaceae* species as key 1,4-dioxane metabolizers (He et al., 2017, 2018; Y.-M. Kim et al., 2009) and cometabolizers (D. Deng et al., 2018; F. Li et al., 2020; Mahendra & Alvarez-Cohen, 2006; Masuda et al., 2012). Interestingly, a previously isolated strain of ethene-oxidizing *Mycobacterium chubuense* (NBB4) was found to contain four distinct SDIMOs representing groups 3, 4, and 6, providing for considerable metabolic diversity (Cheung et al., 2013; Coleman et al., 2011; Le & Coleman, 2011). While only two potentially *Mycobacteria*-associated SDIMOs were found here, this adds to evidence suggesting that they are a metabolically versatile, environmentally widespread taxon with great importance in SDIMO-mediated cometabolism.

*Mycobacteria* are also relevant in research areas concerning water health due to their potential pathogenicity and ubiquity in the water environment. *Mycobacteria* are generally able to survive in stressful environments due to their oligotrophic lifestyle and capacity for biofilm

formation, both features which would enable their adaptation and persistence in BAC communities (Percival & Williams, 2014). We searched our samples for *Mycobacterium* species associated with human infections and found significant enrichment of *M. tuberculosis*, *M. avium*, and *M. goodii* in propane-dosed media samples compared to control samples. These opportunistic pathogens have previously been found in low abundances in GAC microbial communities (H. Wang et al., 2013) and may pose a risk of infection to immunocompromised individuals through aerosols. Pathogen removal barriers following biofiltration such as UV disinfection and disinfectant addition in this particular train should ensure the removal of potentially enriched Mycobacteria sloughed from BAC biofilms. Informed decision-making about the relevance of these findings to water health would require culture confirmation of the presence of these species since metagenomically-assigned taxonomic data can be unreliable, but the apparent enrichment of potentially pathogenic strains clearly poses an area for further research prior to widespread implementation of this technology. Specifically, potential airborne exposure at the facility through air scouring of biofilters warrants further investigation into quantity and identity of these mycobacterial species.

### **3.4.2 SDIMOs**

Highly diverse SDIMOs were found in all samples, even those samples which were not exposed to propane. SDIMOs have been found in widely distributed environments, including Arctic groundwater and uncontaminated environmental samples and soils (Coleman et al., 2006; He et al., 2018; M. Li et al., 2013). It is therefore unsurprising that such a variety of SDIMOs were identified in these samples, suggesting that augmentation of biofilters with SDIMO-harboring bacteria is unnecessary and stimulation of native microorganisms could enrich dioxane cometabolizers in most water treatment systems. In this system, ozonation directly upstream of biofiltration prevents introduction of microorganisms into the biofilter, which may also contribute to the stability of SDIMO-harboring Mycobacterial communities in the biofilters.

The use of untargeted metagenomics-based sequencing offered unbiased detection of all six SDIMO subgroups, though the aromatic-degrading subgroups (1, 2, and 5) displayed higher richness than the aliphatic-preferring subgroups (groups 3, 4, and 6). The two most abundant SDIMOs identified through metagenomic functional gene analysis were most closely related to the propane/toluene and phenol/toluene monooxygenases. These two subgroups have been previously reported to predominantly oxidize aromatic compounds (Holmes & Coleman, 2008).

Aside from 1,4-dioxane, aromatic-oxidizing SDIMOs are known to degrade a wide variety of contaminants upon cometabolic stimulation, including chlorinated solvents, gasoline oxygenates such as MTBE, and NDMA (Chen et al., 2023; Chu et al., 2018; Sharp et al., 2007). NDMA is a contaminant of emerging concern generated during ozonation that may experience enhanced removal because of SDIMO enrichment and activation. However, all four biofilters in this study (including the controls) demonstrated consistent removal of NDMA to below detection limits, possibly due to the action of diverse low-level SDIMOs in the control biofilters. In addition, targeted chemical sampling of 1,4-dioxane prevented any conclusions about the removal of other CECs in this system. Despite this limitation, the hypothesis remains that other potable reuse trains facing contamination with diverse trace organic contaminants aside from dioxane may benefit from the enrichment of Group 1 and 2 SDIMOs with propane or another primary substrate.

### **3.4.3 Lag phases and starvation**

Initial acclimation of BAC communities to propane amendment appeared to involve a lag phase between observation of high relative abundances of *Mycobacteria* in the biofilter effluent (observed in effluent in July 2022) and initial cometabolic 1,4-dioxane removal (observed in late August 2022). This lag period supports the notion that mere abundance of SDIMOs is not sufficient for cometabolic removal – the involved microorganisms require consistent exposure to the provided primary substrate before cometabolism can begin. This is also evidenced by the lag phase experienced during the second start-up of propane amendment after the operational failure. Reasons for this lag phase may include a need for the *Mycobacteria*-rich biofilms to mature and develop on the surface of the BAC before significant cometabolic activity is seen, or a need for constant exposure to propane for SDIMOs to be activated.

BAC communities from the dosed biofilters significantly changed during the starvation period. While still enriched compared to control samples, relative abundances of *Mycobacterium* and *Mycolicibacterium* decreased (Figure 3.5). Additionally, both total SDIMO abundance and abundances of the two key SDIMOs decreased by about 50%. These observations are consistent with the chemical data which showed loss of cometabolic 1,4-dioxane removal after the disruption. However, one of the biofilters (PROPANE-1) from the final sampling event demonstrated recovery of dioxane cometabolism activity within two weeks of restarting amendment (83% measured dioxane removal). In this same filter, a near-immediate recovery in

total SDIMO abundance occurred within a week of restart. This biofilter was not only dosed with propane, but also provided with phosphoric acid to test the role of phosphorus as a potential limiting nutrient. While ANOSIM tests did not find any significant overall differences in microbial communities between PROPANE-1 and PROPANE-2, it is possible that the provision of phosphate allowed PROPANE-1 to bounce back more quickly than PROPANE-2. PROPANE-1 also had higher overall abundances of SDIMOs throughout the experiment compared to PROPANE-2, though the role of phosphate in this is also uncertain.

Notably, this recovery of cometabolic activity in PROPANE-1 did not coincide with a full recovery in the abundance of the two highly enriched SDIMOs. Instead, another specific SDIMO appeared to drastically increase in abundance. This sequence was identified as a putative Group 3 methane monooxygenase (Figure 3.6, Put. G3). Together, this evidence suggests that the starvation event offered an opportunity for succession in which the many other diverse SDIMO-harboring bacteria competed with the established *Mycobacteriaceae* community when subjected to stress. Despite this, the two originally enriched SDIMOs remained the two most abundant functional genes. Ultimately, observations about this sample are not statistically relevant due to lack of replication, but they do offer insight into the robustness of the overall BAC microbial community attributed to 1) redundancy in contaminant-degrading functional genes and 2) selection for persistent, oligotrophic, biofilm-forming organisms.

### Conclusion

Results from this research show the promise of propane amendment for biological degradation of 1,4-dioxane in water treatment biofilters, especially those in potable reuse systems which require high removal of low influent concentrations of contaminants. Propane-enriched BAC communities and functional gene profiles are distinct from those of non-amended BAC and are dominated by persistent, stable, stress-tolerant organisms such as *Mycobacteriaceae* which may have the potential to cometabolically degrade a variety of aromatic compounds. Diverse SDIMOs are natively present in biofilters, eliminating the need for augmentation of biofilters with metabolically unique organisms for contaminant degradation. While cometabolic degradation is subject to an initial lag phase, established cometabolizing biofilms may be highly stress-tolerant and can readily recover from a starvation period.

### **Supplemental Text 3.1.**

Treatment tertiary-treated wastewater influent in the SWIFT Research Center potable reuse train includes rapid mix with aluminum chlorohydrate and a cationic polymer, flocculation, sedimentation, and ozonation with addition of monochloramine as a bromate formation suppressor. Monochloramine addition results in a dose of approximately 1 mg/L-N of free ammonia to each biofilter. The biofilters consist of 5 feet of f416 media from Calgon Corporation. PROPANE-2, CTRL-1, and CTRL-2 sit atop a sand and gravel underdrain. PROPANE-1 has plastic media retainer underdrain. The BAFs operate at ~220 gpm, with a surface loading rate of ~3 gpm/ft<sup>2</sup>. They backwash on one of 3 parameters: effluent NTU >0.15 NTU, >8 ft of head loss accumulation, or >70 hr run time.

**Supplemental Table 3.1.** Manually curated database of confirmed, well-characterized SDIMOs representing all 6 subfamilies.

<b>SDIMO group</b>	<b>Uniprot ID</b>	<b>Reference</b>	<b>Gene</b>	<b>Description</b>	<b>Organism</b>
Group 1 (toluene, propene)	A0A4Y6KT04	(D. Deng et al., 2020)	tMO	Toluene monooxygenase	Azoarcus sp. DD4
Group 1 (toluene, propene)	O69178	<a href="https://pubmed.ncbi.nlm.nih.gov/9797289/">https://pubmed.ncbi.nlm.nih.gov/9797289/</a>	phlK	Putative hydroxylase component	Cupriavidus necator (Alcaligenes eutrophus) (Ralstonia eutropha JMP134)
Group 1 (toluene, propene)	Q00456	<a href="https://www.uniprot.org/citations/1885512">https://www.uniprot.org/citations/1885512</a>	tmoA	Toluene-4-monooxygenase system, hydroxylase component subunit alpha	Pseudomonas mendocina KR1
Group 1 (toluene, propene)	Q51939	<a href="https://pubmed.ncbi.nlm.nih.gov/7867951/">https://pubmed.ncbi.nlm.nih.gov/7867951/</a>	tbuA1	Alpha hydroxylase subunit	Ralstonia pickettii (Burkholderia pickettii) PKO1
Group 1 (toluene, propene)	O87798	<a href="https://www.ncbi.nlm.nih.gov/pmc/articles/PMC106479/">https://www.ncbi.nlm.nih.gov/pmc/articles/PMC106479/</a>	touA	Toluene o-xylene monooxygenase oxygenase subunit TouA	Stutzerimonas stutzeri (Pseudomonas stutzeri) OX1
Group 1 (toluene, propene)	O87082	<a href="https://www.uniprot.org/citations/CI-1T5S3BI8MTLD8">https://www.uniprot.org/citations/CI-1T5S3BI8MTLD8</a>	XamoA	Alkene monooxygenase system, oxygenase component subunit alpha	Xanthobacter autotrophicus (strain ATCC BAA-1158 / Py2)
Group 1 (toluene, propene)	Q9RBP2	<a href="https://pubmed.ncbi.nlm.nih.gov/10715003/">https://pubmed.ncbi.nlm.nih.gov/10715003/</a>	isoA	propane 2-monooxygenase	Rhodococcus sp. (strain AD45)
Group 1 (toluene, propene)	P95408	<a href="https://www.sciencedirect.com/science/article/abs/pii/S0922338X97869760">https://www.sciencedirect.com/science/article/abs/pii/S0922338X97869760</a>	bmoA	Benzene monooxygenase oxygenase subunit	Pseudomonas aeruginosa J1104
Group 1 (toluene, propene)	Q1LNS7	<a href="https://www.mdpi.com/2076-2607/10/2/484">https://www.mdpi.com/2076-2607/10/2/484</a>	tmoA	Toluene-4-monooxygenase system protein A	Cupriavidus metallidurans (strain ATCC 43123 / DSM 2839 / NBRC 102507 / CH34) (Ralstonia metallidurans)

<b>SDIMO group</b>	<b>Uniprot ID</b>	<b>Reference</b>	<b>Gene</b>	<b>Description</b>	<b>Organism</b>
Group 1 (toluene, propene)	A0A0D3 QM77	<a href="https://www.uniprot.org/citations/25779640">https://www.uniprot.org/citations/25779640</a>	tmoA	toluene 4-monoxygenase (subunit 6/6)	Pseudomonas sp. M4
Group 1 (toluene, propene)	O07068	(Ma & Herson, 2000)	tbhA	Toluene-3-monoxygenase oxygenase subunit 1	Burkholderia cepacia (Pseudomonas cepacia) AA1
Group 1 (toluene, propene)	Q9EZP0	<a href="https://pubmed.ncbi.nlm.nih.gov/11571188/">https://pubmed.ncbi.nlm.nih.gov/11571188/</a>	tbc2A	Tbc2A monoxygenase	Burkholderia cepacia (Pseudomonas cepacia) JS150
Group 2 (phenol, toluene)	Q43981	(Ehrt et al., 1995)	orf4	Phenolhydroxylase component	Acinetobacter calcoaceticus NCIB8250
Group 2 (phenol, toluene)	O32431	<a href="https://academic.oup.com/femsle/article/155/1/99/599243">https://academic.oup.com/femsle/article/155/1/99/599243</a>	dsoD	DMS oxygenase component	Acinetobacter sp strain 20B
Group 2 (phenol, toluene)	Q9ANX2	<a href="https://www.uniprot.org/citations/CI-INJT0KSNDFRPR">https://www.uniprot.org/citations/CI-INJT0KSNDFRPR</a>	tomA3	toluene 2-monoxygenase	Burkholderia cepacia G4
Group 2 (phenol, toluene)	Q9S147	<a href="https://pubmed.ncbi.nlm.nih.gov/10589844/">https://pubmed.ncbi.nlm.nih.gov/10589844/</a>	phcN	Phenol hydroxylase subunit	Comamonas testosteroni (Pseudomonas testosteroni) R5
Group 2 (phenol, toluene)	Q9ZNP4	<a href="https://pubmed.ncbi.nlm.nih.gov/9802031/">https://pubmed.ncbi.nlm.nih.gov/9802031/</a>	aphN	Phenol hydroxylase component	Comamonas testosteroni (Pseudomonas testosteroni) TA441
Group 2 (phenol, toluene)	Q52164	(Herrmann et al., 1995)	phlD	Subunit of phenolhydroxylase	Pseudomonas putida (Arthrobacter siderocapsulatus) strain H
Group 2 (phenol, toluene)	Q52572	<a href="https://pubmed.ncbi.nlm.nih.gov/7574644/">https://pubmed.ncbi.nlm.nih.gov/7574644/</a>	tbmD	toluene/benzene 2-monoxygenase	Pseudomonas sp (Burkholderia cepacia JS150)

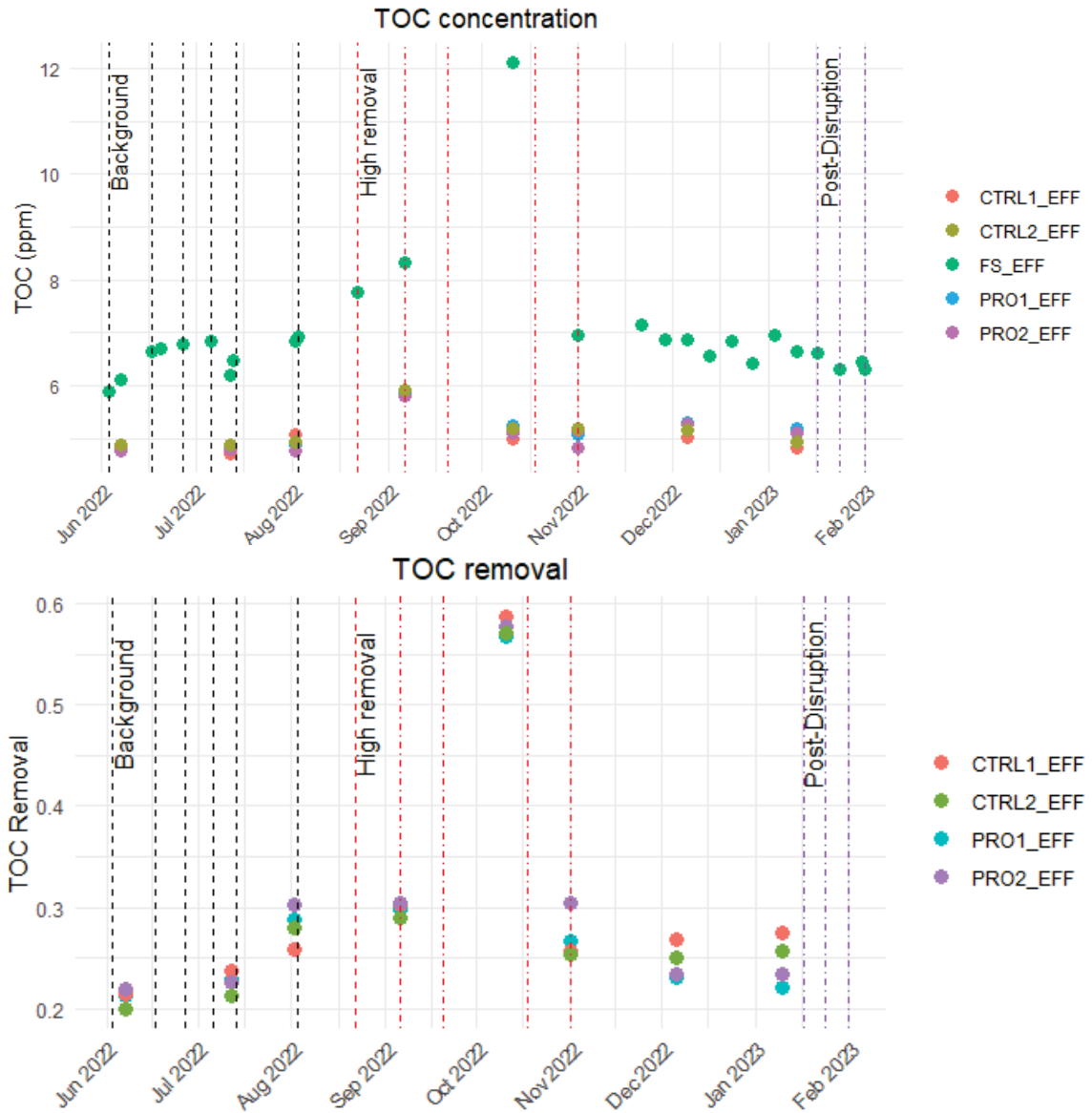
SDIMO group	Uniprot ID	Reference	Gene	Description	Organism
Group 2 (phenol, toluene)	Q9EZP3	<a href="https://pubmed.ncbi.nlm.nih.gov/11571188/">https://pubmed.ncbi.nlm.nih.gov/11571188/</a>	tbc1D	Tbc1D monooxygenase	Pseudomonas sp (Burkholderia cepacia JS150)
Group 2 (phenol, toluene)	P19732	<a href="https://www.uniprot.org/citations/2254258">https://www.uniprot.org/citations/2254258</a>	dmpN	Phenol 2-monooxygenase, oxygenase component DmpN	Pseudomonas sp. (strain CF600)
Group 2 (phenol, toluene)	O84961	<a href="https://pubmed.ncbi.nlm.nih.gov/9695910/">https://pubmed.ncbi.nlm.nih.gov/9695910/</a>	poxD	Phenol hydroxylase component	Ralstonia eutropha E2
Group 2 (phenol, toluene)	Q1LMG3	<a href="https://www.mdpi.com/2076-2607/10/2/484">https://www.mdpi.com/2076-2607/10/2/484</a>	phyC	Phenol hydroxylase P3 protein	Cupriavidus metallidurans (strain ATCC 43123 / DSM 2839 / NBRC 102507 / CH34) (Ralstonia metallidurans)
Group 2 (phenol, toluene)	Q1LNR5	<a href="https://www.mdpi.com/2076-2607/10/2/484">https://www.mdpi.com/2076-2607/10/2/484</a>	tomA3	Toluene hydroxylase P3 protein	Cupriavidus metallidurans (strain ATCC 43123 / DSM 2839 / NBRC 102507 / CH34) (Ralstonia metallidurans)
Group 2 (phenol, toluene)	Q9RAF6	<a href="https://pubmed.ncbi.nlm.nih.gov/16232697/">https://pubmed.ncbi.nlm.nih.gov/16232697/</a>	phyC	Phenol hydroxylase component	Ralstonia sp. KN1
Group 2 (phenol, toluene)	Q52173	<a href="https://pubmed.ncbi.nlm.nih.gov/7828892/">https://pubmed.ncbi.nlm.nih.gov/7828892/</a>	phh	Phenol hydroxylase component	Pseudomonas putida (Arthrobacter siderocapsulatus) P35x
Group 2 (phenol, toluene)	Q8VUT9	<a href="https://www.jstage.jst.go.jp/article/jsme2/18/3/18_3_167/article/-char/ja/">https://www.jstage.jst.go.jp/article/jsme2/18/3/18_3_167/article/-char/ja/</a>	phkD	Phenol hydroxylase subunit PhkD	Paraburkholderia kururiensis subsp. kururiensis KP23
Group 3 (methane, butane)	P22869	<a href="https://www.uniprot.org/citations/2205538">https://www.uniprot.org/citations/2205538</a>	mmoX	methane monooxygenase (soluble) (subunit 6/6)	Methylococcus capsulatus Bath
Group 3 (methane, butane)	O06116	<a href="https://journals.asm.org/doi/pdf/10.1128/">https://journals.asm.org/doi/pdf/10.1128/</a>	mmoX	Soluble methane monooxygenase protein A alpha subunit	Methylocystis sp. M

SDIMO group	Uniprot ID	Reference	Gene	Description	Organism
		<a href="#">aem.63.5.1898-1904.1997</a>			
Group 3 (methane, butane)	Q9RAM3	<a href="https://journals.asm.org/doi/pdf/10.1128/aem.65.9.3929-3935.1999">https://journals.asm.org/doi/pdf/10.1128/aem.65.9.3929-3935.1999</a>	mmoX	soluble methane monooxygenase	Methylcystis sp. WI14
Group 3 (methane, butane)	Q7DJP7	<a href="https://journals.asm.org/doi/pdf/10.1128/AEM.65.12.5198-5206.1999">https://journals.asm.org/doi/pdf/10.1128/AEM.65.12.5198-5206.1999</a>	mmoX	Soluble methane monooxygenase hydroxylase component (MMOH) alpha subunit	Methylomonas sp. KSPIII
Group 3 (methane, butane)	P27353	<a href="https://www.uniprot.org/citations/1904125">https://www.uniprot.org/citations/1904125</a>	mmoX	methane monooxygenase (soluble) (subunit 6/6)	Methylosinus trichosporium OB3b
Group 3 (methane, butane)	E1CBX4	<a href="https://academic.oup.com/femsle/article/312/1/71/470786">https://academic.oup.com/femsle/article/312/1/71/470786</a>	mmoX	methane monooxygenase (soluble)	Methylovulum miyakonense
Group 4 (ethene, propene)	Q53027	<a href="https://citeseerx.ist.psu.edu/document?repid=rep1&amp;type=pdf&amp;doi=35da00b8c771a6dc8dd20f31e46b48dcc039ffd00">https://citeseerx.ist.psu.edu/document?repid=rep1&amp;type=pdf&amp;doi=35da00b8c771a6dc8dd20f31e46b48dcc039ffd00</a>	amoC	propane 2-monooxygenase	Gordonia rubripertincta (Rhodococcus corallinus) B-276
Group 4 (ethene, propene)	D2K2E0	<a href="https://www.uniprot.org/citations/CI-2LMCUSF8DN6F2">https://www.uniprot.org/citations/CI-2LMCUSF8DN6F2</a>	EtnC	Ethene monooxygenase	Mycobacterium chubuense strain NBB4
Group 5 (propane, THF)	Q768T5	<a href="https://www.uniprot.org/citations/21183637">https://www.uniprot.org/citations/21183637</a>	prmA	Propane 2-monooxygenase, hydroxylase component large subunit	Gordonia sp. (strain TY-5)
Group 5 (propane, THF)	A0QTU8	<a href="https://www.uniprot.org/citations/21183637">https://www.uniprot.org/citations/21183637</a>	mimA	Propane 2-monooxygenase, hydroxylase component large subunit	Mycolicibacterium smegmatis (strain ATCC 700084 / mc(2)155) (Mycobacterium smegmatis)

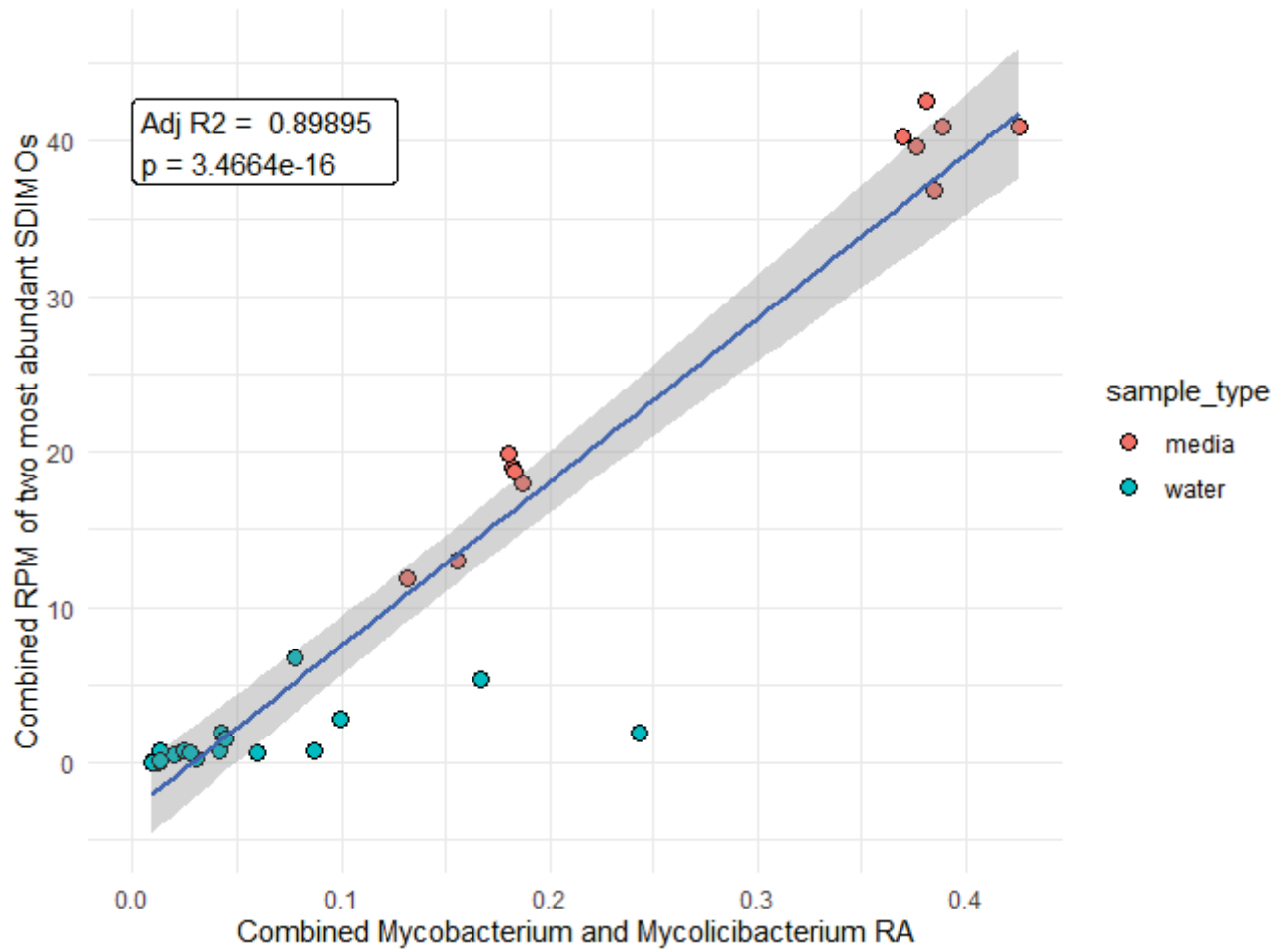
<b>SDIMO group</b>	<b>Uniprot ID</b>	<b>Reference</b>	<b>Gene</b>	<b>Description</b>	<b>Organism</b>
Group 5 (propane, THF)	Q0SJK9	<a href="https://www.uniprot.org/citations/17873074">https://www.uniprot.org/citations/17873074</a>	prmA	Propane 2-monooxygenase, hydroxylase component large subunit	Rhodococcus jostii (strain RHA1)
Group 5 (propane, THF)	Q9F3V6	<a href="https://pubmed.ncbi.nlm.nih.gov/12632259/">https://pubmed.ncbi.nlm.nih.gov/12632259/</a>	thmA	propane 2-monooxygenase / tetrahydrofuran MO	Pseudonocardia tetrahydrofuranoxydans K1
Group 5 (propane, THF)	N/A	<a href="https://escholarship.org/content/qt7xq1r0kd/qt7xq1r0kd.pdf?t=mtfc43&amp;v=lg">https://escholarship.org/content/qt7xq1r0kd/qt7xq1r0kd.pdf?t=mtfc43&amp;v=lg</a>	thmA	thf monooxygenase	Pseudonocardia dioxanivorans CB1190
Group 5 (propane, THF)	E9RFS9	<a href="https://www.uniprot.org/citations/21183637">https://www.uniprot.org/citations/21183637</a>	mimA	Propane 2-monooxygenase, hydroxylase component large subunit	Mycobacterium goodii (Mycolicibacterium goodii)
Group 5 (propane, THF)	Q08KD8	<a href="https://www.uniprot.org/citations/17046531">https://www.uniprot.org/citations/17046531</a>	prm2A	propane 2-monooxygenase (subunit 4/4)	Pseudonocardia sp. TY-7
Group 5 (propane, THF)	Q08KE2	<a href="https://www.uniprot.org/citations/17046531">https://www.uniprot.org/citations/17046531</a>	prm1A	propane 2-monooxygenase (subunit 4/4)	Pseudonocardia sp. TY-7
Group 6 (propane)	A0A1Y0CHK1	<a href="https://pubs.acs.org/doi/full/10.1021/acs.estlett.7b00456">https://pubs.acs.org/doi/full/10.1021/acs.estlett.7b00456</a>	prmA	propane 2-monooxygenase	Mycobacterium dioxanotrophicus PH-06
Group 6 (propane)	Q08KF2	<a href="https://www.uniprot.org/citations/17046531">https://www.uniprot.org/citations/17046531</a>	prmA	propane 2-monooxygenase	Mycobacterium sp. TY-6
Group 6 (propane)	I7DAA5	<a href="https://academic.oup.com/lambio/article/5/3/175/6704905">https://academic.oup.com/lambio/article/5/3/175/6704905</a>	prmA	propane 2-monooxygenase	Mycobacterium Sp. Strain ENV421

**Supplemental Table 3.2.** Conserved SDIMO motifs which were used to filter putative SDIMO sequences from false positive sequences identified through blastp. Approximate start and end locations are based on locations within the consensus SDIMO sequence of all sequences in the database.

	APPROXIMATE START LOCATION	APPROXIMATE END LOCATION	LENGTH	PATTERN	CONSENSUS SEQUENCE	PUTATIVE FUNCTION
<b>MOTIF 1</b>	69	86	18	[DE]-x(2)-[KR]-x(5)- Y-x(3)-[QE]-x(2)-K- [DE]	DPFKLTMDEYXKMQREKD	unconfirmed
<b>MOTIF 2</b>	156	160	5	D-[DE]-x-R-H	DELRH	iron-binding (confirmed)
<b>MOTIF 3</b>	224	229	6	E-x(3)-T-N	ETVFTN	Proton delivery to active site
<b>MOTIF 4</b>	253	261	9	S-x(3)-D-E-x-R-H	SIQSDESRH	iron-binding (confirmed)
<b>MOTIF 5</b>	342	350	9	[LM]-x(3)-G-x(3)-P	LERYGLRKP	Docking



**Supplemental Figure 3.1.** TOC concentration and removal fraction over the course of the study in all four biofilters. Removal in each biofilter was measured relative to the TOC concentration in Floc/Sed effluent (FS\_EFF).



**Supplemental Figure 3.2.** Linear correlation between the combined relative abundance of *Mycobacterium* and *Mycolicibacterium* and the quantity of the two most abundant SDIMOs in reads per million total reads.

## References

- Adamson, D. T., Piña, E. A., Cartwright, A. E., Rauch, S. R., Hunter Anderson, R., Mohr, T., & Connor, J. A. (2017). 1,4-Dioxane drinking water occurrence data from the third unregulated contaminant monitoring rule. *Science of The Total Environment*, 596–597, 236–245. <https://doi.org/10.1016/j.scitotenv.2017.04.085>
- Arbizu, P. M. (2017). *pairwiseAdonis: Pairwise Multilevel Comparison using Adonis*.
- Babcock, N., Dickenson, E., Gerrity, D., Papp, K., Quinones, O., & Khan, E. (2022). The role of ammonia oxidizing microorganisms in biofiltration for the removal of trace organic compounds in secondary wastewater effluent. *Environmental Science: Water Research & Technology*, 8(12), 2994–3006. <https://doi.org/10.1039/D2EW00662F>
- Bacaro, F., Dickenson, E., A. Trenholm, R., & Gerrity, D. (2019). N -Nitrosodimethylamine (NDMA) formation and mitigation in potable reuse treatment trains employing ozone and biofiltration. *Environmental Science: Water Research & Technology*, 5(4), 713–725. <https://doi.org/10.1039/C8EW00926K>
- Barajas-Rodriguez, F. J., & Freedman, D. L. (2018). Aerobic biodegradation kinetics for 1,4-dioxane under metabolic and cometabolic conditions. *Journal of Hazardous Materials*, 350, 180–188. <https://doi.org/10.1016/j.jhazmat.2018.02.030>
- Bell, C. H., Wong, J., Parsons, K., Semel, W., McDonough, J., & Gerber, K. (2022). First Full-Scale In Situ Propane Biosparging for Co-Metabolic Bioremediation of 1,4-Dioxane. *Groundwater Monitoring & Remediation*, 42(4), 54–66. <https://doi.org/10.1111/gwmr.12511>
- Bolyen, E., Rideout, J. R., Dillon, M. R., Bokulich, N. A., Abnet, C. C., Al-Ghalith, G. A., Alexander, H., Alm, E. J., Arumugam, M., Asnicar, F., Bai, Y., Bisanz, J. E., Bittinger, K., Brejnrod, A., Brislawn, C. J., Brown, C. T., Callahan, B. J., Caraballo-Rodríguez, A. M., Chase, J., ... Caporaso, J. G. (2019). Reproducible, interactive, scalable and extensible microbiome data science using QIIME 2. *Nature Biotechnology*, 37(8), 852–857. <https://doi.org/10.1038/s41587-019-0209-9>
- Boon, N., Pycke, B. F. G., Marzorati, M., & Hammes, F. (2011). Nutrient gradients in a granular activated carbon biofilter drives bacterial community organization and dynamics. *Water Research*, 45(19), 6355–6361. <https://doi.org/10.1016/j.watres.2011.09.016>
- Buchfink, B., Xie, C., & Huson, D. H. (2015). Fast and sensitive protein alignment using DIAMOND. *Nature Methods*, 12(1), Article 1. <https://doi.org/10.1038/nmeth.3176>
- Bushnell, B. (2014). *BBMap: A Fast, Accurate, Splice-Aware Aligner* (Patent LBNL-7065E). <https://www.osti.gov/biblio/1241166>
- Camper, A. K., LeChevallier, M. W., Broadaway, S. C., & McFeters, G. A. (1985). Evaluation of procedures to desorb bacteria from granular activated carbon. *Journal of Microbiological Methods*, 3(3), 187–198. [https://doi.org/10.1016/0167-7012\(85\)90046-6](https://doi.org/10.1016/0167-7012(85)90046-6)
- Canada, K. A., Iwashita, S., Shim, H., & Wood, T. K. (2002). Directed Evolution of Toluene ortho-Monooxygenase for Enhanced 1-Naphthol Synthesis and Chlorinated Ethene Degradation. *Journal of Bacteriology*, 184(2), 344–349. <https://doi.org/10.1128/jb.184.2.344-349.2002>
- Chen, S., Zhou, Y., Chen, Y., & Gu, J. (2018). fastp: An ultra-fast all-in-one FASTQ preprocessor. *Bioinformatics*, 34(17), i884–i890. <https://doi.org/10.1093/bioinformatics/bty560>
- Chen, Y., Ren, H., Kong, X., Wu, H., & Lu, Z. (2023). A multicomponent propane monooxygenase catalyzes the initial degradation of methyl tert -butyl ether in *Mycobacterium vaccae* JOB5. *Applied and Environmental Microbiology*, 89(10), e01187-23. <https://doi.org/10.1128/aem.01187-23>

Cheung, S., McCarl, V., Holmes, A. J., Coleman, N. V., & Rutledge, P. J. (2013). Substrate range and enantioselectivity of epoxidation reactions mediated by the ethene-oxidising Mycobacterium strain NBB4. *Applied Microbiology and Biotechnology*, *97*(3), 1131–1140. <https://doi.org/10.1007/s00253-012-3975-6>

Chu, M.-Y. J., Bennett, P. J., Dolan, M. E., Hyman, M. R., Peacock, A. D., Bodour, A., Anderson, R. H., Mackay, D. M., & Goltz, M. N. (2018). Concurrent Treatment of 1,4-Dioxane and Chlorinated Aliphatics in a Groundwater Recirculation System Via Aerobic Cometabolism. *Groundwater Monitoring & Remediation*, *38*(3), 53–64. <https://doi.org/10.1111/gwmmr.12293>

Coleman, N. V., Bui, N. B., & Holmes, A. J. (2006). Soluble di-iron monooxygenase gene diversity in soils, sediments and ethene enrichments. *Environmental Microbiology*, *8*(7), 1228–1239. <https://doi.org/10.1111/j.1462-2920.2006.01015.x>

Coleman, N. V., Yau, S., Wilson, N. L., Nolan, L. M., Migocki, M. D., Ly, M., Crossett, B., & Holmes, A. J. (2011). Untangling the multiple monooxygenases of Mycobacterium chubuense strain NBB4, a versatile hydrocarbon degrader. *Environmental Microbiology Reports*, *3*(3), 297–307. <https://doi.org/10.1111/j.1758-2229.2010.00225.x>

Colorado DPHE. (2013). *5 CCR 1002-41*. [www.sos.state.co.us/CCR/GenerateRulePdf.do?ruleVersionId=5034&fileName=5%20CCR%201002-41](http://www.sos.state.co.us/CCR/GenerateRulePdf.do?ruleVersionId=5034&fileName=5%20CCR%201002-41).

Dalton, H., Stirling, D. I., Quayle, J. R., Higgins, I. J., Quayle, J. R., & Bull, A. T. (1997). Co-metabolism. *Philosophical Transactions of the Royal Society of London. B, Biological Sciences*, *297*(1088), 481–496. <https://doi.org/10.1098/rstb.1982.0056>

Deng, D., Li, F., & Li, M. (2018). A Novel Propane Monooxygenase Initiating Degradation of 1,4-Dioxane by Mycobacterium dioxanotrophicus PH-06. *Environmental Science & Technology Letters*, *5*(2), 86–91. <https://doi.org/10.1021/acs.estlett.7b00504>

Deng, D., Pham, D. N., Li, F., & Li, M. (2020). Discovery of an Inducible Toluene Monooxygenase That Cooxidizes 1,4-Dioxane and 1,1-Dichloroethylene in Propanotrophic Azoarcus sp. Strain DD4. *Applied and Environmental Microbiology*, *86*(17), e01163-20. <https://doi.org/10.1128/AEM.01163-20>

Deng, Y., & Zhao, R. (2015). Advanced Oxidation Processes (AOPs) in Wastewater Treatment. *Current Pollution Reports*, *1*(3), 167–176. <https://doi.org/10.1007/s40726-015-0015-z>

DeSantis, T. Z., Hugenholtz, P., Larsen, N., Rojas, M., Brodie, E. L., Keller, K., Huber, T., Dalevi, D., Hu, P., & Andersen, G. L. (2006). Greengenes, a Chimera-Checked 16S rRNA Gene Database and Workbench Compatible with ARB. *Applied and Environmental Microbiology*, *72*(7), 5069–5072. <https://doi.org/10.1128/AEM.03006-05>

Doherty, A.-C., Lee, C.-S., Meng, Q., Sakano, Y., Noble, A. E., Grant, K. A., Esposito, A., Gobler, C. J., & Venkatesan, A. K. (2023). Contribution of household and personal care products to 1,4-dioxane contamination of drinking water. *Current Opinion in Environmental Science & Health*, *31*, 100414. <https://doi.org/10.1016/j.coesh.2022.100414>

Ehrt, S., Schirmer, F., & Hillen, W. (1995). Genetic organization, nucleotide sequence and regulation of expression of genes encoding phenol hydroxylase and catechol 1,2-dioxygenase in Acinetobacter calcoaceticus NCIB8250. *Molecular Microbiology*, *18*(1), 13–20. [https://doi.org/10.1111/j.1365-2958.1995.mmi\\_18010013.x](https://doi.org/10.1111/j.1365-2958.1995.mmi_18010013.x)

EPA IRIS. (2013). *1,4-Dioxane Chemical Assessment Summary* (CASRN 123-91-1). U.S. Environmental Protection Agency National Center for Environmental Assessment. [https://iris.epa.gov/static/pdfs/0326\\_summary.pdf](https://iris.epa.gov/static/pdfs/0326_summary.pdf)

- Fu, L., Niu, B., Zhu, Z., Wu, S., & Li, W. (2012). CD-HIT: Accelerated for clustering the next-generation sequencing data. *Bioinformatics*, *28*(23), 3150–3152. <https://doi.org/10.1093/bioinformatics/bts565>
- Fuchs, G., Boll, M., & Heider, J. (2011). Microbial degradation of aromatic compounds—From one strategy to four. *Nature Reviews Microbiology*, *9*(11), 803–816. <https://doi.org/10.1038/nrmicro2652>
- Gerrity, D., Gamage, S., Holady, J. C., Mawhinney, D. B., Quiñones, O., Trenholm, R. A., & Snyder, S. A. (2011). Pilot-scale evaluation of ozone and biological activated carbon for trace organic contaminant mitigation and disinfection. *Water Research*, *45*(5), 2155–2165. <https://doi.org/10.1016/j.watres.2010.12.031>
- Gerrity, D., Owens-Bennett, E., Venezia, T., Stanford, B. D., Plumlee, M. H., Debroux, J., & Trussell, R. S. (2014). Applicability of Ozone and Biological Activated Carbon for Potable Reuse. *Ozone: Science & Engineering*, *36*(2), 123–137. <https://doi.org/10.1080/01919512.2013.866886>
- Godri Pollitt, K. J., Kim, J.-H., Peccia, J., Elimelech, M., Zhang, Y., Charkoftaki, G., Hodges, B., Zucker, I., Huang, H., Deziel, N. C., Murphy, K., Ishii, M., Johnson, C. H., Boissevain, A., O’Keefe, E., Anastas, P. T., Orlicky, D., Thompson, D. C., & Vasiliou, V. (2019). 1,4-Dioxane as an emerging water contaminant: State of the science and evaluation of research needs. *Science of The Total Environment*, *690*, 853–866. <https://doi.org/10.1016/j.scitotenv.2019.06.443>
- Goff, K. L., & Hug, L. A. (2022). Environmental Potential for Microbial 1,4-Dioxane Degradation Is Sparse despite Mobile Elements Playing a Role in Trait Distribution. *Applied and Environmental Microbiology*, *88*(7), e02091-21. <https://doi.org/10.1128/aem.02091-21>
- Guidelines for Water Reuse. (2004). U.S. Environmental Protection Agency.
- Hazen, T. C. (2018). Cometabolic Bioremediation. In R. Steffan (Ed.), *Consequences of Microbial Interactions with Hydrocarbons, Oils, and Lipids: Biodegradation and Bioremediation* (pp. 1–15). Springer International Publishing. [https://doi.org/10.1007/978-3-319-44535-9\\_5-1](https://doi.org/10.1007/978-3-319-44535-9_5-1)
- He, Y., Mathieu, J., da Silva, M. L. B., Li, M., & Alvarez, P. J. J. (2018). 1,4-Dioxane-degrading consortia can be enriched from uncontaminated soils: Prevalence of Mycobacterium and soluble di-iron monooxygenase genes. *Microbial Biotechnology*, *11*(1), 189–198. <https://doi.org/10.1111/1751-7915.12850>
- He, Y., Mathieu, J., Yang, Y., Yu, P., da Silva, M. L. B., & Alvarez, P. J. J. (2017). 1,4-Dioxane Biodegradation by Mycobacterium dioxanotrophicus PH-06 Is Associated with a Group-6 Soluble Di-Iron Monooxygenase. *Environmental Science & Technology Letters*, *4*(11), 494–499. <https://doi.org/10.1021/acs.estlett.7b00456>
- Herrmann, H., Müller, C., Schmidt, I., Mahnke, J., Petruschka, L., & Hahnke, K. (1995). Localization and organization of phenol degradation genes of Pseudomonas putida strain H. *Molecular & General Genetics: MGG*, *247*(2), 240–246. <https://doi.org/10.1007/BF00705655>
- Hogard, S., Salazar-Benites, G., Pearce, R., Nading, T., Schimmoller, L., Wilson, C., Heisig-Mitchell, J., & Bott, C. (2021). Demonstration-scale evaluation of ozone–biofiltration–granular activated carbon advanced water treatment for managed aquifer recharge. *Water Environment Research*, *93*(8), 1157–1172. <https://doi.org/10.1002/wer.1525>
- Holmes, A. J. (2009). The Diversity of Soluble Di-iron Monooxygenases with Bioremediation Applications. In A. Singh, R. C. Kuhad, & O. P. Ward (Eds.), *Advances in Applied Bioremediation* (pp. 91–102). Springer. [https://doi.org/10.1007/978-3-540-89621-0\\_5](https://doi.org/10.1007/978-3-540-89621-0_5)

Holmes, A. J., & Coleman, N. V. (2008). Evolutionary ecology and multidisciplinary approaches to prospecting for monooxygenases as biocatalysts. *Antonie van Leeuwenhoek*, *94*(1), 75–84. <https://doi.org/10.1007/s10482-008-9227-1>

Hyatt, D., Chen, G.-L., LoCascio, P. F., Land, M. L., Larimer, F. W., & Hauser, L. J. (2010). Prodigal: Prokaryotic gene recognition and translation initiation site identification. *BMC Bioinformatics*, *11*(1), 119. <https://doi.org/10.1186/1471-2105-11-119>

Inoue, D., Hisada, K., Okumura, T., Yabuki, Y., Yoshida, G., Kuroda, M., & Ike, M. (2020). Carbon sources that enable enrichment of 1,4-dioxane-degrading bacteria in landfill leachate. *Biodegradation*, *31*(1), 23–34. <https://doi.org/10.1007/s10532-019-09891-w>

Inoue, D., Tsunoda, T., Sawada, K., Yamamoto, N., Saito, Y., Sei, K., & Ike, M. (2016). 1,4-Dioxane degradation potential of members of the genera *Pseudonocardia* and *Rhodococcus*. *Biodegradation*, *27*(4), 277–286. <https://doi.org/10.1007/s10532-016-9772-7>

Kim, T. G., Kim, S.-H., & Cho, K.-S. (2014). Effects of ultrasonic pretreatment on quantity and composition of bacterial DNA recovered from granular activated carbon used for drinking water treatment. *Journal of Environmental Science and Health, Part A*, *49*(5), 609–616. <https://doi.org/10.1080/10934529.2014.859469>

Kim, Y.-M., Jeon, J.-R., Murugesan, K., Kim, E.-J., & Chang, Y.-S. (2009). Biodegradation of 1,4-dioxane and transformation of related cyclic compounds by a newly isolated *Mycobacterium* sp. PH-06. *Biodegradation*, *20*(4), 511–519. <https://doi.org/10.1007/s10532-008-9240-0>

Kirtane, A., Atkinson, J. D., & Sassoubre, L. (2020). Design and Validation of Passive Environmental DNA Samplers Using Granular Activated Carbon and Montmorillonite Clay. *Environmental Science & Technology*, *54*(19), 11961–11970. <https://doi.org/10.1021/acs.est.0c01863>

Le, N. B., & Coleman, N. V. (2011). Biodegradation of vinyl chloride, cis-dichloroethene and 1,2-dichloroethane in the alkene/alkane-oxidising *Mycobacterium* strain NBB4. *Biodegradation*, *22*(6), 1095–1108. <https://doi.org/10.1007/s10532-011-9466-0>

Leahy, J. G., Batchelor, P. J., & Morcomb, S. M. (2003). Evolution of the soluble diiron monooxygenases. *FEMS Microbiology Reviews*, *27*(4), 449–479. [https://doi.org/10.1016/S0168-6445\(03\)00023-8](https://doi.org/10.1016/S0168-6445(03)00023-8)

Lee, C.-S., Asato, C., Wang, M., Mao, X., Gobler, C. J., & Venkatesan, A. K. (2021). Removal of 1,4-dioxane during on-site wastewater treatment using nitrogen removing biofilters. *Science of The Total Environment*, *771*, 144806. <https://doi.org/10.1016/j.scitotenv.2020.144806>

Li, D., Liu, C.-M., Luo, R., Sadakane, K., & Lam, T.-W. (2015). MEGAHIT: An ultra-fast single-node solution for large and complex metagenomics assembly via succinct *de Bruijn* graph. *Bioinformatics*, *31*(10), 1674–1676. <https://doi.org/10.1093/bioinformatics/btv033>

Li, F., Deng, D., & Li, M. (2020). Distinct Catalytic Behaviors between Two 1,4-Dioxane-Degrading Monooxygenases: Kinetics, Inhibition, and Substrate Range. *Environmental Science & Technology*, *54*(3), 1898–1908. <https://doi.org/10.1021/acs.est.9b05671>

Li, M., Mathieu, J., Yang, Y., Fiorenza, S., Deng, Y., He, Z., Zhou, J., & Alvarez, P. J. J. (2013). Widespread Distribution of Soluble Di-Iron Monooxygenase (SDIMO) Genes in Arctic Groundwater Impacted by 1,4-Dioxane. *Environmental Science & Technology*, *47*(17), 9950–9958. <https://doi.org/10.1021/es402228x>

Lippincott, D. (2015). Bioaugmentation and Propane Biosparging for In Situ Biodegradation of 1,4-Dioxane. *Groundwater Monitoring & Remediation*, *35*(2), 81–92. <https://doi.org/10.1111/gwmr.12093>

- Love, M. I., Huber, W., & Anders, S. (2014). Moderated estimation of fold change and dispersion for RNA-seq data with DESeq2. *Genome Biology*, *15*(12), 550. <https://doi.org/10.1186/s13059-014-0550-8>
- Lu, J., Breitwieser, F. P., Thielen, P., & Salzberg, S. L. (2017). Bracken: Estimating species abundance in metagenomics data. *PeerJ Computer Science*, *3*, e104. <https://doi.org/10.7717/peerj-cs.104>
- Lu, J., & Salzberg, S. L. (2020). Ultrafast and accurate 16S rRNA microbial community analysis using Kraken 2. *Microbiome*, *8*(1), 124. <https://doi.org/10.1186/s40168-020-00900-2>
- Lu, Z., Sun, W., Li, C., Cao, W., Jing, Z., Li, S., Ao, X., Chen, C., & Liu, S. (2020). Effect of granular activated carbon pore-size distribution on biological activated carbon filter performance. *Water Research*, *177*, 115768. <https://doi.org/10.1016/j.watres.2020.115768>
- Ma, Y., & Herson, D. S. (2000). The catechol 2,3-dioxygenase gene and toluene monooxygenase genes from Burkholderia sp. AA1, an isolate capable of degrading aliphatic hydrocarbons and toluene. *Journal of Industrial Microbiology and Biotechnology*, *25*(3), 127–131. <https://doi.org/10.1038/sj.jim.7000042>
- Mahendra, S., & Alvarez-Cohen, L. (2006). Kinetics of 1,4-Dioxane Biodegradation by Monooxygenase-Expressing Bacteria. *Environmental Science & Technology*, *40*(17), 5435–5442. <https://doi.org/10.1021/es060714v>
- Malaeb, L., & Ayoub, G. M. (2011). Reverse osmosis technology for water treatment: State of the art review. *Desalination*, *267*(1), 1–8. <https://doi.org/10.1016/j.desal.2010.09.001>
- Masuda, H., McClay, K., Steffan, R. J., & Zylstra, G. J. (2012). Characterization of three propane-inducible oxygenases in Mycobacterium sp. Strain ENV421. *Letters in Applied Microbiology*, *55*(3), 175–181. <https://doi.org/10.1111/j.1472-765X.2012.03290.x>
- McElroy, A. C., Ogles, M. E., Hyman, M. R., & Knappe, D. R. U. (2023). Pilot-scale biofiltration of 1,4-dioxane at drinking water-relevant concentrations. *Water Research*, *231*, 119652. <https://doi.org/10.1016/j.watres.2023.119652>
- Mohr, T. K. G., DiGuseppi, W. H., Hatton, J. W., & Anderson, J. K. (2020). *Environmental Investigation and Remediation: 1,4-Dioxane and other Solvent Stabilizers, Second Edition*. CRC Press.
- Nichol, T., Murrell, J. C., & Smith, T. J. (2015). Controlling the Activities of the Diiron Centre in Bacterial Monooxygenases: Lessons from Mutagenesis and Biodiversity. *European Journal of Inorganic Chemistry*, *2015*(21), 3419–3431. <https://doi.org/10.1002/ejic.201500043>
- Nishijima, W., & Speitel, G. E. (2004). Fate of biodegradable dissolved organic carbon produced by ozonation on biological activated carbon. *Chemosphere*, *56*(2), 113–119. <https://doi.org/10.1016/j.chemosphere.2004.03.009>
- Notomista, E., Lahm, A., Di Donato, A., & Tramontano, A. (2003). Evolution of Bacterial and Archaeal Multicomponent Monooxygenases. *Journal of Molecular Evolution*, *56*(4), 435–445. <https://doi.org/10.1007/s00239-002-2414-1>
- Oh, S., Hammes, F., & Liu, W.-T. (2018). Metagenomic characterization of biofilter microbial communities in a full-scale drinking water treatment plant. *Water Research*, *128*, 278–285. <https://doi.org/10.1016/j.watres.2017.10.054>
- Oksanen, J., Simpson, G. L., Blanchet, F. G., Kindt, R., Legendre, P., Minchin, P. R., O’Hara, R. B., Solymos, P., Stevens, M. H. H., Szoecs, E., Wagner, H., Barbour, M., Bedward, M., Bolker, B., Borcard, D., Carvalho, G., Chirico, M., Caceres, M. D., Durand, S., ... Weedon, J. (2022). *vegan: Community Ecology Package*. <https://CRAN.R-project.org/package=vegan>

- Otto, M., & Nagaraja, S. (2007). Treatment technologies for 1,4-Dioxane: Fundamentals and field applications. *Remediation Journal*, 17(3), 81–88. <https://doi.org/10.1002/rem.20135>
- Percival, S. L., & Williams, D. W. (2014). Chapter Nine—Mycobacterium. In S. L. Percival, M. V. Yates, D. W. Williams, R. M. Chalmers, & N. F. Gray (Eds.), *Microbiology of Waterborne Diseases (Second Edition)* (pp. 177–207). Academic Press. <https://doi.org/10.1016/B978-0-12-415846-7.00009-3>
- Pérez-Pantoja, D., Donoso, R., Junca, H., González, B., & Pieper, D. H. (2010). Phylogenomics of Aerobic Bacterial Degradation of Aromatics. In K. N. Timmis (Ed.), *Handbook of Hydrocarbon and Lipid Microbiology* (pp. 1355–1397). Springer. [https://doi.org/10.1007/978-3-540-77587-4\\_95](https://doi.org/10.1007/978-3-540-77587-4_95)
- Polasko, A. L., Miao, Y., Kwok, I., Park, K., Park, J. O., & Mahendra, S. (2021). Vinyl chloride and 1,4-dioxane metabolism by *Pseudonocardia dioxanivorans* CB1190. *Journal of Hazardous Materials Letters*, 2, 100039. <https://doi.org/10.1016/j.hazl.2021.100039>
- Sales, C. M., Grostern, A., Parales, J. V., Parales, R. E., & Alvarez-Cohen, L. (2013). Oxidation of the Cyclic Ethers 1,4-Dioxane and Tetrahydrofuran by a Monooxygenase in Two *Pseudonocardia* Species. *Applied and Environmental Microbiology*, 79(24), 7702–7708. <https://doi.org/10.1128/AEM.02418-13>
- Salimi, M., Esrafil, A., Gholami, M., Jonidi Jafari, A., Rezaei Kalantary, R., Farzadkia, M., Kermani, M., & Sobhi, H. R. (2017). Contaminants of emerging concern: A review of new approach in AOP technologies. *Environmental Monitoring and Assessment*, 189(8), 414. <https://doi.org/10.1007/s10661-017-6097-x>
- Sharp, J. O., Sales, C. M., LeBlanc, J. C., Liu, J., Wood, T. K., Eltis, L. D., Mohn, W. W., & Alvarez-Cohen, L. (2007). An Inducible Propane Monooxygenase Is Responsible for N-Nitrosodimethylamine Degradation by *Rhodococcus* sp. Strain RHA1. *Applied and Environmental Microbiology*, 73(21), 6930–6938. <https://doi.org/10.1128/AEM.01697-07>
- Stohr, H., Vaidya, R., Wilson, C., Pruden, A., Salazar-Benites, G., & Bott, C. (2023). Cometabolic Treatment of 1,4-Dioxane in Biologically Active Carbon Filtration with Tetrahydrofuran and Propane at Relevant Concentrations for Potable Reuse. *ACS ES&T Water*, 3(9), 2948–2954. <https://doi.org/10.1021/acsestwater.3c00182>
- Summers, R. S., Shiokari, S. T., Johnson, S., Peterson, E., Yu, Y., & Cook, S. (2020). Reuse treatment with ozonation, biofiltration, and activated carbon adsorption for total organic carbon control and disinfection byproduct regulation compliance. *AWWA Water Science*, 2(5), e1190. <https://doi.org/10.1002/aws2.1190>
- Sundaram, V., Pagilla, K., Guarin, T., Li, L., Marfil-Vega, R., & Bukhari, Z. (2020). Extended field investigations of ozone-biofiltration advanced water treatment for potable reuse. *Water Research*, 172, 115513. <https://doi.org/10.1016/j.watres.2020.115513>
- Taboada, B., Estrada, K., Ciria, R., & Merino, E. (2018). Operon-mapper: A web server for precise operon identification in bacterial and archaeal genomes. *Bioinformatics*, 34(23), 4118–4120. <https://doi.org/10.1093/bioinformatics/bty496>
- Takada Hoshino, Y., & Matsumoto, N. (2005). Skim Milk Drastically Improves the Efficacy of DNA Extraction from Andisol, a Volcanic Ash Soil. *Japan Agricultural Research Quarterly: JARQ*, 39(4), 247–252. <https://doi.org/10.6090/jarq.39.247>
- Takada-Hoshino, Y., & Matsumoto, N. (2004). An Improved DNA Extraction Method Using Skim Milk from Soils That Strongly Adsorb DNA. *Microbes and Environments*, 19(1), 13–19. <https://doi.org/10.1264/jsme2.19.13>

The UniProt Consortium. (2023). UniProt: The Universal Protein Knowledgebase in 2023. *Nucleic Acids Research*, 51(D1), D523–D531. <https://doi.org/10.1093/nar/gkac1052>

Trigodet, F., Lolans, K., Fogarty, E., Shaiber, A., Morrison, H. G., Barreiro, L., Jabri, B., & Eren, A. M. (2022). High molecular weight DNA extraction strategies for long-read sequencing of complex metagenomes. *Molecular Ecology Resources*, 22(5), 1786–1802. <https://doi.org/10.1111/1755-0998.13588>

Vaidya, R., Wilson, C. A., Salazar-Benites, G., Pruden, A., & Bott, C. (2020). Implementing Ozone-BAC-GAC in potable reuse for removal of emerging contaminants. *AWWA Water Science*, 2(5), e1203. <https://doi.org/10.1002/aws2.1203>

Vatankhah, H., Szczuka, A., Mitch, W. A., Almaraz, N., Brannum, J., & Bellona, C. (2019). Evaluation of Enhanced Ozone–Biologically Active Filtration Treatment for the Removal of 1,4-Dioxane and Disinfection Byproduct Precursors from Wastewater Effluent. *Environmental Science & Technology*, 53(5), 2720–2730. <https://doi.org/10.1021/acs.est.8b06897>

Vera, G. A. de, Gerrity, D., Stoker, M., Frehner, W., & C. Wert, E. (2018). Impact of upstream chlorination on filter performance and microbial community structure of GAC and anthracite biofilters. *Environmental Science: Water Research & Technology*, 4(8), 1133–1144. <https://doi.org/10.1039/C8EW00115D>

Vilchez-Vargas, R., Junca, H., & Pieper, D. H. (2010). Metabolic networks, microbial ecology and ‘omics’ technologies: Towards understanding in situ biodegradation processes. *Environmental Microbiology*, 12(12), 3089–3104. <https://doi.org/10.1111/j.1462-2920.2010.02340.x>

Volossiouk, T., Robb, E. J., & Nazar, R. N. (1995). Direct DNA extraction for PCR-mediated assays of soil organisms. *Applied and Environmental Microbiology*, 61(11), 3972–3976. <https://doi.org/10.1128/aem.61.11.3972-3976.1995>

Walters, W., Hyde, E. R., Berg-Lyons, D., Ackermann, G., Humphrey, G., Parada, A., Gilbert, J. A., Jansson, J. K., Caporaso, J. G., Fuhrman, J. A., Apprill, A., & Knight, R. (2015). Improved Bacterial 16S rRNA Gene (V4 and V4-5) and Fungal Internal Transcribed Spacer Marker Gene Primers for Microbial Community Surveys. *mSystems*, 1(1), 10.1128/msystems.00009-15. <https://doi.org/10.1128/msystems.00009-15>

Wang, H., Pryor, M. A., Edwards, M. A., Falkinham, J. O., & Pruden, A. (2013). Effect of GAC pre-treatment and disinfectant on microbial community structure and opportunistic pathogen occurrence. *Water Research*, 47(15), 5760–5772. <https://doi.org/10.1016/j.watres.2013.06.052>

Wang, L. K., Pereira, N. C., & Hung, Y.-T. (Eds.). (2004). *Handbook of environmental engineering*. Humana Press.

Weber, Jr., W., Pirbazari, M., & Melson, G. (1978). Biological growth on activated carbon: An investigation by scanning electron microscopy. *Environmental Science & Technology*, 12(7), 817–819. <https://doi.org/10.1021/es60143a005>

Weidhaas, J. L., Zigmund, M. J., & Dupont, R. R. (2012). Aerobic Biotransformation of N-Nitrosodimethylamine and N-Nitrodimethylamine by Benzene-, Butane-, Methane-, Propane-, and Toluene-Fed Cultures. *Bioremediation Journal*, 16(2), 74–85. <https://doi.org/10.1080/10889868.2012.665961>

Xiong, Y., Mason, O. U., Lowe, A., Zhang, Z., Zhou, C., Chen, G., Villalonga, M. J., & Tang, Y. (2020). Investigating promising substrates for promoting 1,4-dioxane biodegradation: Effects of ethane and tetrahydrofuran on microbial consortia. *Biodegradation*, 31(3), 171–182. <https://doi.org/10.1007/s10532-020-09901-2>

Xu, L., Canales, M., Zhou, Q., Karu, K., Zhou, X., Su, J., Campos, L. C., & Ciric, L. (2023). Antibiotic resistance genes and the association with bacterial community in biofilms occurring during the drinking water granular activated carbon (GAC) sandwich biofiltration. *Journal of Hazardous Materials*, 460, 132511. <https://doi.org/10.1016/j.jhazmat.2023.132511>

Zenker, M. J., Borden, R. C., & Barlaz, M. A. (2004, July 6). *Modeling Cometabolism of Cyclic Ethers* (world) [Research-article]. <https://Home.Liebertpub.Com/Ees>; Mary Ann Liebert, Inc. <https://doi.org/10.1089/109287502760271535>

Zhang, D., Li, W., Zhang, S., Liu, M., Zhao, X., & Zhang, X. (2011). Bacterial Community and Function of Biological Activated Carbon Filter in Drinking Water Treatment. *Biomedical and Environmental Sciences*, 24(2), 122–131. <https://doi.org/10.3967/0895-3988.2011.02.006>

Zhang, S., Gedalanga, P. B., & Mahendra, S. (2017). Advances in bioremediation of 1,4-dioxane-contaminated waters. *Journal of Environmental Management*, 204, 765–774. <https://doi.org/10.1016/j.jenvman.2017.05.033>

Zhou, Z., Xu, L., Zhu, L., Liu, Y., Shuai, X., Lin, Z., & Chen, H. (2021). Metagenomic analysis of microbiota and antibiotic resistome in household activated carbon drinking water purifiers. *Environment International*, 148, 106394. <https://doi.org/10.1016/j.envint.2021.106394>